10

Electromagnetic properties of disperse media

The purpose of this chapter consists in considering basic electromagnetic characteristics of disperse media, which are widespread in the terrestrial atmosphere. The basic notions are introduced for quantitative absorption and scattering characteristics of both secluded particles and disperse media having the form of clouds of independent, randomly located scatterers. The principal concepts of Mie scattering theory and approximations used in practice, such as Rayleigh scattering, resonance scattering, and geometric optics approximation, are presented in the chapter. The basic characteristics describing the mechanical disperse properties of heterogeneous mixtures are introduced. The absorbing and scattering properties of natural polydisperse media, containing water drops and water particles in various phase states, are considered. The chapter presents a rich set of experimental findings on the absorption and scattering characteristics of disperse media spread in the terrestrial atmosphere. The main attention is given to the analysis of electromagnetic characteristics intended for studying the scattering and absorption processes in disperse media, in the microwave band predominantly. The basic results are presented of investigation of highly concentrated disperse media included absorbing scatterers in the microwave band.

10.1 ELECTROMAGNETIC PROPERTIES OF SECLUDED PARTICLES

From the viewpoint of radiative transfer theory, of principal interest for us are the transmission and scattering characteristics of an electromagnetic wave in the presence of a cloud of randomly located, electromagnetically independent scatterers. We shall analyse this problem in this chapter in two stages. First, we shall consider a secluded particle and study its scattering and absorption characteristics. At the second stage we shall take into account the contributions of a great number of non-correlated particles and derive the general relations for a wave propagating in

a cloud of randomly distributed particles. The first of these stages – the analysis of characteristics of a secluded particle – is described in this section. This issue has been exhaustively elucidated in a series of publications (Stratton, 1941; Shifrin, 1951, 1968, 1971; Hulst, 1981; Born and Wolf, 1999; Deirmendjian, 1969; Ishimaru, 1978; Bohren and Hoffman, 1983; Ivazyn, 1991). For this reason, we shall consider here only the basic physical approaches to this complicated problem as applied to microwave sensing tasks.

10.1.1 The scattering cross-section and the scattering amplitude

When a secluded and solitary particle is irradiated by the electromagnetic wave, some part of the incident power is scattered and leaves a particle irrevocably, and the other part is absorbed and transforms into heat eventually. These two basic phenomena – scattering and absorption – can be described most conveniently by supposing the particle to be illuminated by a planar incident wave.

Consider a linearly polarized planar electromagnetic wave propagating in a medium with relative dielectric and magnetic permittivities equal to unity. The electric field of such a wave has a form (see section 1.6):

$$\mathbf{E}_{\mathrm{i}}(\mathbf{r}, \boldsymbol{\Omega}') = E_0 \mathbf{e}_{\mathrm{i}} \exp\left[\mathrm{j}k(\boldsymbol{\Omega}'\mathbf{r})\right] \tag{10.1}$$

Here E_0 is the field amplitude; $k = 2\pi/\lambda$ is the wave number, λ is the wavelength in a medium (external with respect to a particle), $\boldsymbol{\Omega}'$ is the unit vector in the direction of propagation of an external field, and $\mathbf{e}_{\mathrm{i}}$ is the unit vector specifying the direction of the external field polarization.

This wave falls on a particle (Figure 10.1) with relative dielectric permittivity ε_{p}, which is complex, generally speaking, and depends on the coordinates, since the particle can be absorbing and inhomogeneous. The field at distant R, measured from some point inside a particle in the direction of unit vector $\boldsymbol{\Omega}$, is equal to the sum of field $\mathbf{E}_{\mathrm{i}}$ of an incident wave and a field $\mathbf{E}_{\mathrm{S}}$ of a wave scattered on a particle. At distances $R > D^2/\lambda$ (D is the characteristic size of a particle, for example, its diametre) owing to the interference of waves coming from various points of a particle, the amplitude and phase of field $\mathbf{E}_{\mathrm{S}}$ vary in a very complicated manner (the so-called near field mode) (see section 5.2). In this case the observation point $\mathbf{r}$ is said to be in the near zone of a particle. For $R > D^2/\lambda$ the scattered field $\mathbf{E}_{\mathrm{S}}$ behaves as a spherical wave and can be presented in the form

$$\mathbf{E}_{\mathrm{S}}(R) = \dot{\boldsymbol{f}}(\bar{\boldsymbol{\Omega}}', \boldsymbol{\Omega}) \frac{\exp(\mathrm{j}kR)}{R}; R > \frac{D^2}{\lambda}, \tag{10.2}$$

where the scattering amplitude $\boldsymbol{f}(\boldsymbol{\Omega}, \boldsymbol{\Omega}')$ describes the amplitude, phase and polarization of a scattered wave in the far zone in the observation direction $\boldsymbol{\Omega}$ provided that the planar wave, propagating in the irradiation direction $\boldsymbol{\Omega}'$, falls on a particle. It should be noted that even in the case of linear polarization of an incident wave the scattered wave of a particle of complicated shape would possess elliptical polarization, generally speaking. The scattering amplitude is very important, because its

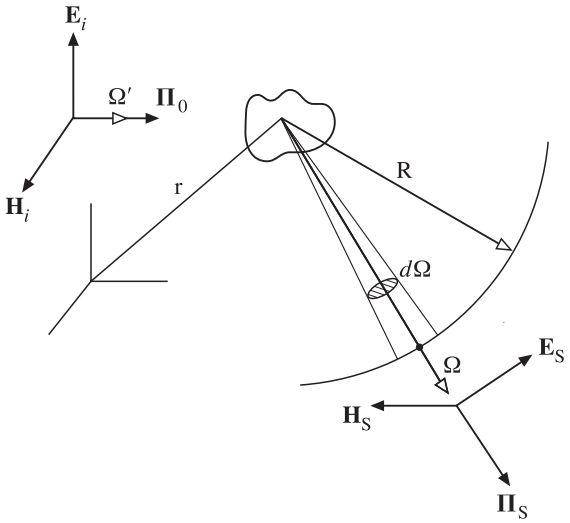

Figure 10.1. Schematic presentation of the geometry in scattering studies in particles. Notation is explained in the text.

value contains information on internal dielectric properties, geometrical shape and size of a particle.

Consider now the density $\mathbf{\Pi}_S$ of a flux of power (see section 1.6), scattered in the directions of wave $\mathbf{\Omega}$ at distance R from a particle, when the wave with power flux density $\mathbf{\Pi}_0$ falls on a particle from the direction $\mathbf{\Omega}'$. Here $\mathbf{\Pi}_0$ and $\mathbf{\Pi}_S$ are the vectors of a power flux density of incident and scattered waves in the corresponding directions:

$$\mathbf{\Pi}_0 = \frac{|\mathbf{E}_i|^2}{2Z_0}\mathbf{\Omega}'; \mathbf{\Pi}_S = \frac{|\mathbf{E}_S|^2}{2Z_0}\mathbf{\Omega}, \tag{10.3}$$

where Z_0 is the characteristic impedance of a medium (see section 1.6). The total power P (measured in watts), which will be scattered by a particle into the ambient space, can be determined as

$$P_S(\mathbf{\Omega}') = \iint_{4\pi} |\mathbf{\Pi}_S(\mathbf{\Omega}', \mathbf{\Omega})| \, d\Omega \tag{10.4}$$

and then the ratio

$$\sigma_S(\mathbf{\Omega}') = \frac{P_S(\mathbf{\Omega}')}{|\mathbf{\Pi}_0|} \tag{10.5}$$

is called the integral scattering cross-section of a particle. It can easily be seen that this value has the dimension of m^2. The physical sense of the introduced quantity consists in the fact that it indicates the difference in losses for power scattering by a particle with respect to its geometrical cross-section (or its geometrical shadow). If the particle has a complicated shape, then the total scattering cross-section depends on the direction from which the external radiation falls on a particle.

Now we introduce another important definition characterizing the power and spatial-angular scattering of incident external radiation, falling on a solitary particle, by this particle. The differential scattering cross-section of a particle is determined as follows:

$$\sigma_{\mathrm{d}}(\boldsymbol{\Omega}', \boldsymbol{\Omega}) = \lim_{R\to\infty}\left[R^2 \frac{|\boldsymbol{\Pi}_{\mathrm{S}}|}{|\boldsymbol{\Pi}_0|}\right] = |\dot{\boldsymbol{f}}(\boldsymbol{\Omega}', \boldsymbol{\Omega})|^2. \tag{10.6}$$

It follows from expression (10.6) that $\sigma_{\mathrm{d}}(\boldsymbol{\Omega}', \boldsymbol{\Omega})$ has the dimension of area divided by a solid angle. Note that the differential scattering cross-section has unambiguous physical sense only when the considered distances from a particle exceed the size of a far zone. In the opposite case (or in the presence of some other particle near the investigated one) the physical unambiguity of the introduced definition is lost.

In radar and scatterometric applications the bistatical radar scattering cross-section σ_{B} and backscattering cross-section σ_{BS} are often used. They are related to $\sigma_{\mathrm{d}}(\boldsymbol{\Omega}', \boldsymbol{\Omega})$ by equations

$$\sigma_{\mathrm{B}}(\boldsymbol{\Omega}', \boldsymbol{\Omega}) = 4\pi\sigma_{\mathrm{d}}(\boldsymbol{\Omega}', \boldsymbol{\Omega}); \sigma_{\mathrm{BS}} = 4\pi\sigma_{\mathrm{d}}(\boldsymbol{\Omega}', -\boldsymbol{\Omega}'). \tag{10.7}$$

Quantity σ_{BS} is also called the radar scattering cross-section. The physical sense of these definitions can be elucidated as follows. Suppose that within the limits of the total solid angle of 4π the power flux density is constant and equals the value of the density for the direction $\boldsymbol{\Omega}$. Then the cross-section of a plate, from which such a power is scattered, is equal to the value of σ_{d} for the direction $\boldsymbol{\Omega}$ multiplied by 4π. Note that the other definitions of backscattering cross-section are sometimes used as well (Skolnik, 1980).

10.1.2 The absorption cross-section

Now we shall consider that part of an incident flux energy, falling on a particle, which will be completely absorbed by a particle and then will transfer into heat. Certainly, if a particle is inhomogeneous in its electromagnetic properties, then all diffraction phenomena arising inside a particle should be taken into account in calculating the absorption. For some unification of the description of scattering and absorption processes the following definition is introduced. By the absorption cross-section $\sigma_{\mathrm{A}}(\boldsymbol{\Omega}')$ is meant the ratio of the total power P_{A}, which was absorbed in particle's volume, to the density of the flux power, which falls on a particle from the direction $\boldsymbol{\Omega}'$,

$$\sigma_{\mathrm{A}}(\boldsymbol{\Omega}') = \frac{P_{\mathrm{A}}}{|\Pi_0(\boldsymbol{\Omega}')|} \tag{10.8}$$

The dimension of the absorption cross-section is expressed in m^2. If a particle is inhomogeneous in its composition, then the absorption cross-section will depend on the direction of incident external radiation. Since the question is about the absorption of electromagnetic energy, this quantity can have no direct relation to the geometry of a particle.

10.1.3 The extinction cross-section

Now we shall consider the following important point. Since we have noted that the energy scattered by a particle is considered in the far zone of a particle, this part of energy 'leaves' a particle irrevocably. Thus, no statistical bond exists between the power absorbed by a particle and the power scattered by the same particle. Only under this condition can one introduce the definition describing the total losses (or extinction) of a particle in the form of a sum of losses for scattering and absorption:

$$\sigma_{\mathrm{E}}(\boldsymbol{\Omega}') = \sigma_{\mathrm{S}}(\boldsymbol{\Omega}') + \sigma_{\mathrm{A}}(\boldsymbol{\Omega}'). \tag{10.9}$$

Quantity $\sigma_{\mathrm{E}}(\boldsymbol{\Omega}')$ is called the extinction cross-section (or the total cross-section).

10.1.4 The single scattering albedo

The relation between absorption and scattering processes, which occur when a particle is irradiated by a flux of electromagnetic radiation, is undoubtedly, a very important factor in studying the total energy balance in transforming (or extracting) the energy of a basic external flux by a particle. The ratio of the extinction scattering cross-section to the total cross-section is called the single scattering albedo of a solitary particle:

$$\omega(\boldsymbol{\Omega}') = \frac{\sigma_{\mathrm{S}}(\boldsymbol{\Omega}')}{\sigma_{\mathrm{S}}(\boldsymbol{\Omega}') + \sigma_{\mathrm{A}}(\boldsymbol{\Omega}')}. \tag{10.10}$$

For natural media the value of albedo varies within very wide limits. So, for optically transparent media in the terrestrial atmosphere (drops of water), the value of albedo is close to unity (0.95–0.99). In the microwave band the albedo of water particles lies within the limits of 0.01–0.8 (Oguchi, 1983), whereas for particles, close in their electromagnetic properties to the black body (such as the hollow water spheres), the albedo is virtually zero (Raizer and Sharkov, 1981).

Note that the albedo of a unit of medium's volume introduced earlier (see section 9.2–9.3) can essentially differ from the albedo of a solitary particle, since the first of these definitions depends on the polydisperse composition of a medium or, in other words, on the relationship between the working wavelength and the range of particles' sizes.

10.1.5 The scattering indicatrix

It is obvious from physical considerations, that any particle of complicated shape will scatter incident radiation in space in an inhomogeneous manner. To describe the character of a spatial–angular scattering on a particle the special dimensionless function $p(\boldsymbol{\Omega}', \boldsymbol{\Omega})$ is introduced, which is the called the scattering indicatrix, in the following form:

$$p(\boldsymbol{\Omega}', \boldsymbol{\Omega}) = 4\pi \frac{\sigma_{\mathrm{d}}(\boldsymbol{\Omega}', \boldsymbol{\Omega})}{\sigma_{\mathrm{E}}(\boldsymbol{\Omega}')}. \tag{10.11}$$

The dimensionless quantity $p(\mathbf{\Omega}', \mathbf{\Omega})$ is sometimes called the phase function and is widely used in radiative transfer theory (in the optical band especially). Note that this name has purely historical roots. Physically, the phase function describes the scattered power and has no relation to the phase of an incident wave (see equation (10.2)). The term 'phase function' arose in astronomy and is related to the phases of the Moon (Ishimaru, 1978).

Using relations (10.6), (10.10) and (10.11), we obtain the equations which associate all the electromagnetic parameters of a particle introduced above:

$$\sigma_{\mathrm{S}}(\mathbf{\Omega}') = \iint_{4\pi} \sigma_{\mathrm{d}}(\mathbf{\Omega}', \mathbf{\Omega})\, \mathrm{d}\Omega = \iint_{4\pi} |\dot{f}(\mathbf{\Omega}', \mathbf{\Omega})|^2\, \mathrm{d}\Omega$$

$$= \frac{\sigma_{\mathrm{E}}(\mathbf{\Omega}')}{4\pi} \iint_{4\pi} p(\mathbf{\Omega}', \mathbf{\Omega})\, \mathrm{d}\Omega, \tag{10.12}$$

$$\omega(\mathbf{\Omega}') = \frac{\sigma_{\mathrm{S}}}{\sigma_{\mathrm{E}}} = \frac{1}{\sigma_{\mathrm{E}}} \iint_{4\pi} |\dot{f}(\mathbf{\Omega}', \mathbf{\Omega})|^2\, \mathrm{d}\Omega = \frac{1}{4\pi} \iint_{4\pi} p(\mathbf{\Omega}', \mathbf{\Omega})\, \mathrm{d}\Omega. \tag{10.13}$$

These relations clear up the physical sense of the introduced parameter – the scattering indicatrix. Suppose that the particle will scatter uniformly within the total solid angle 4π surrounding it, i.e. $p(\mathbf{\Omega}', \mathbf{\Omega}) = 1$. Then particle's albedo will be equal to unity, and the total cross-section of the particle will be determined by its scattering cross-section only. In such a case the particle is called purely scattering.

Note that the aforementioned approach to forming the scattering indicatrix of a particle is not unique. There are, however, other approaches to the definition of a scattering indicatrix (Skolnik, 1980). Then relations (10.12) and (10.13) will have other numerical coefficients.

10.1.6 The optical theorem

The extinction cross-section describes total power losses in an incident wave caused by wave scattering and absorption in a particle. It is important to note that a close relationship has been found to exist between the behaviour of a wave, scattered in the forward direction, and the extinction cross-section. The appropriate general relation forms the content of the so-called optical theorem, or the forwards scattering theorem. The optical theorem states that the extinction cross-section is related to an imaginary part of the forwards scattering amplitude $\boldsymbol{f}(\mathbf{\Omega}', \mathbf{\Omega})$, and this relation has a form (Born and Wolf, 1999):

$$\sigma_{\mathrm{E}} = \frac{4\pi}{k} \operatorname{Im} \dot{\boldsymbol{f}}(\mathbf{\Omega}', \mathbf{\Omega}) \mathbf{e}_{\mathrm{i}}, \tag{10.14}$$

where Im implies 'the imaginary part', and $\mathbf{e}_{\mathrm{i}}$ is the unit vector characterizing the direction of polarization of an incident wave.

This theorem is often used for theoretical calculations of the extinction cross-section when the scattering amplitude is known. The application of this theorem is rather difficult in the experimental respect, since it requires separating an incident

external flux from the radiation scattered by a particle 'forwards'. Note that in quantum theory there exists a full analogue of the theorem mentioned, which associates the imaginary part of the amplitude of elastic forwards scattering with the total cross-section of a particle at scattering on the other particle (Prochorov, 1984).

10.1.7 Integral presentations of scattering amplitude and absorption cross-section

The mathematical description of a scattering amplitude and scattering and absorption cross-sections can be accomplished in one of two ways. For simple-shaped bodies, such as a sphere or an infinite cylinder, the accurate expressions for the mentioned quantities can be found. The accurate solution for a homogeneous dielectric sphere, which is called the Mie solution (or the Mie theory), will be considered in section 10.2. However, in the majority of practically important cases the shape of particles is not simple. For this reason, a number of techniques have been developed, allowing us to obtain the values of unknown cross-sections proceeding from integral presentations of a scattering amplitude (Ishimaru, 1978).

Considering the field in the far zone, scattered by a particle, and knowing the field inside a particle $\mathbf{E}(\mathbf{r})$, one can obtain from the solutions of Maxwell's equations the following integral expression for the scattering amplitude of an inhomogeneous particle:

$$\dot{\mathbf{f}}(\boldsymbol{\Omega}', \boldsymbol{\Omega}) = \frac{k^2}{4\pi} \int_V \{-\boldsymbol{\Omega} \times [\boldsymbol{\Omega} \times \mathbf{E}(\mathbf{r})]\} \{\dot{\varepsilon}(\mathbf{r}) - 1\} \exp(-\mathrm{j}k\mathbf{r}\boldsymbol{\Omega})\, \mathrm{d}V. \tag{10.15}$$

This is the accurate expression for a scattering amplitude $\boldsymbol{f}(\boldsymbol{\Omega}', \boldsymbol{\Omega})$ in terms of the total electric field $\mathbf{E}(\mathbf{r})$ inside a particle. Note that the double vector product inside the integral represents a component of the scattered field perpendicular to $\boldsymbol{\Omega}$ for any direction of a vector of the total electric field $\mathbf{E}(\mathbf{r})$ inside a particle (Figure 10.2). The main difficulty of the procedure considered consists in the fact that, strictly speaking, the total electric field $\mathbf{E}(\mathbf{r})$ inside a particle is unknown; as a result, expression (10.15) does not provide a closed description of a scattering amplitude in terms of known

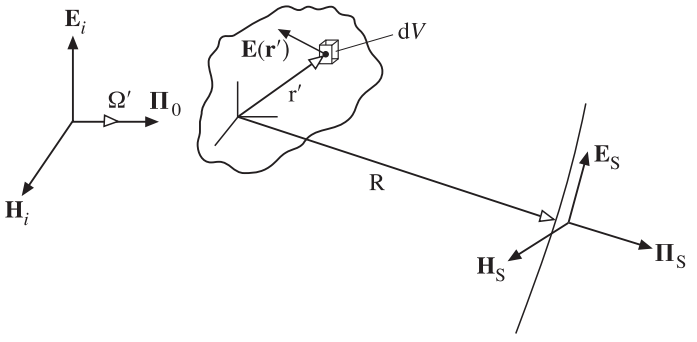

Figure 10.2. The geometrical positions of the point within the particle (r') and the observation point (R) studies of scattering amplitude. Notation is explained in the text.

quantities. However, in many practically important cases the field $\mathbf{E}(\mathbf{r})$ can approximately be replaced by some known function and, thus, one can obtain the useful approximate expression for the scattering amplitude of complicated particles, such as spheroids or multi-layered spheres (Bhandari, 1985; Rysakov and Ston, 2001).

In its turn, the absorption cross-section of any dielectric body represents a volume integral of losses inside a particle:

$$\sigma_{\mathrm{A}} = k \int_V \varepsilon_2(\mathbf{r}) |\mathbf{E}(\mathbf{r})|^2 \, \mathrm{d}V. \tag{10.16}$$

In this expression the incident wave amplitude is chosen to be equal to unity.

Expressions (10.15) and (10.16) are the accurate integral expressions for the scattering amplitude and for the absorption cross-section in terms of unknown total field $\mathbf{E}(\mathbf{r})$ inside a particle.

10.2 BASIC CONCEPTS OF MIE THEORY

The important problem in electromagnetic radiation scattering by material particles consists in finding the relationship between the properties (i.e. the size, shape, dielectric characteristics) of particles to the angular distribution of scattered radiation and to the external radiation absorption by particles. Such a problem arises in many fields of science and technology (such as astrophysics, biochemistry, radiophysics, optical oceanography). For this reason, numerous theoretical and experimental investigations have been carried out to study electromagnetic wave scattering. Historically, such investigations were first been carried out in the optical band and then were spread to the IR and radio wavelength bands.

One of first researchers, J. Rayleigh, proceeding from purely dimensional considerations, obtained the famous asymptotic approximate solution for radiation scattering by spherical particles whose size is small as compared to the wavelength of incident radiation falling on the particle. This work was followed by the general theory of radiation absorption and scattering by homogeneous particles having simple geometrical shape, such as a sphere or a circular cylinder. This theory was formulated by G. Mie in 1908. In the Mie theory, based on the solution of fundamental Maxwell's equations, the idealized situation was considered, namely, a simple spherical particle made of a homogeneous, isotropic material and placed in a homogeneous, isotropic, dielectric, boundless medium and irradiated by planar waves propagating in a particular direction. A purely dielectric spherical particle does not absorb radiation, whereas an electrically conducting spherical particle partially absorbs, partially scatters and partially transmits the incident radiation. The derivation of Mie's solution, as well as the mathematical and physical aspects of his theory, including the features of numerical calculation algorithms, are contained in a series of books (Stratton, 1941; Shifrin, 1951, 1968, 1971; Hulst, 1981; Born and Wolf, 1999; Deirmendjian, 1969; Ozisik, 1973; Ishimaru, 1978; Ivazyn, 1991). The solutions for the amplitude of a scattered wave for a sphere have a form of complicated series containing the Riccati–Bessel functions and the

Riccati–Hankel functions of increasing order. The results of Mie's solution are most useful for determining absorption and scattering coefficients, as well as the scattering indicatrix for spherical particles suspended in a dielectric medium, provided that the particles are spaced at a rather great distance from each other. Some special experiments were carried out for determining the minimum distance between spherical particles ensuring their independent scattering. It was found that for some optical scatterers the mutual interference can be neglected if the distance between the centres of spherical particles is greater than three diametres. In the majority of applied problems (the studies of cloudy systems, snowfalls, aerosols) the particles are separated by much greater distances from each other. Note, however, that in the Mie theory the idealized case is considered, namely, a secluded spherical particle, which acts as an independent point-like scatterer in a boundless medium, whereas the scatterers met with in the majority of practical applications have an arbitrary geometrical shape. At present, great efforts are being made to study electromagnetic radiation scattering by particles of arbitrary shape and orientation and complicated structure (such as multilayer particles, spheroids) (Bhandari, 1985; Rysakov and Ston, 2001). Nevertheless, we shall consider below the results of Mie's theory, since this is a unique fundamental theory now available, and its results are useful in many idealized cases.

10.2.1 Parameters of the Mie theory

A series of dimensionless parameters are introduced in the theory, which are widely used in practice.

The ratio of cross-section values, introduced above, to the geometrical cross-section is called the efficiency factor and designated by Q_{i}, where i is equal to A, S or E (which means absorption, scattering or extinction, respectively). Thus, one can write

$$Q_{\mathrm{i}} = \frac{\sigma_{\mathrm{i}}}{\pi a^2}, \tag{10.17}$$

where a is the radius of a sphere. As follows from (10.9), the efficiency factors satisfy the relation

$$Q_{\mathrm{E}} = Q_{\mathrm{S}} + Q_{\mathrm{A}}. \tag{10.18}$$

By the size parameter is meant the ratio of the length of circumference of a studied sphere to the working wavelength $x(0 < x < \infty)$

$$x = \frac{2\pi a}{\lambda} = \frac{\pi D}{\lambda}, \tag{10.19}$$

where D is the diameter of a sphere.

The complex parameter m of refraction of sphere's substance relative to dielectric properties of an ambient boundless space is

$$\dot{m} = \frac{\dot{n}_{\mathrm{SP}}}{\dot{n}_{\mathrm{S}}} = n + \mathrm{j}\chi. \tag{10.20}$$

Here n_{SP} is the index of refraction of sphere's substance, and n_S is a similar characteristic of the ambient space. If the ambient space is not a vacuum, but a medium with a high value of n_S, then parameter $|m|$ can be less than unity. For example, such a situation takes place in studying the propagation and scattering of electromagnetic waves of the optical band in a marine medium in the presence of air bubbles.

Since the sphere is a symmetrical particle, the scattering does not depend on an azimuthal angle, but is a function of scattering angle θ_0 concluded between the directions of incident and scattered beams. Thus, we introduced one more parameter – the scattering angle. Here it is necessary to keep in mind, that if the incident flux possesses strictly linear polarization, then the (secondary) radiation, scattered by a sphere, acquires the character of elliptically polarized radiation (Stratton, 1941), and its description requires bringing in the azimuthal angle. If, however, the primary field is non-polarized (the case of natural thermal radiation), then the secondary radiation is weakly polarized. This makes it possible to present the scattering indicatrix in the form of series over the Legendre polynomials

$$p(\cos\theta_0) = 1 + \sum_{j=1}^{\infty} A_j P_j(\cos\theta_0), \tag{10.21}$$

where θ_0 is the scattering angle, $P_j(\cos\theta_0)$ are the Legendre polynomials, A_j are expansion coefficients, which are functions of parameter x and parameter of refraction only.

To get an idea about the results of the Mie theory, we shall write the expressions for the efficiency factors of extinction and of scattering, which can be presented in the form of infinite series:

$$Q_E = \frac{2}{x^2}\sum_{n=1}^{\infty}(2n+1)\{\mathrm{Re}\,(\dot{a}_n + \dot{b}_n)\}, \tag{10.22}$$

$$Q_S = \frac{2}{x^2}\sum_{n=1}^{\infty}(2n+1)\{|\dot{a}_n|^2 + |\dot{b}_n|^2\}, \tag{10.23}$$

where Re is the real part of a sum. If the particle does not absorb the incident radiation (i.e. the index of refraction is a real number and the particle is a pure scatterer), then expressions (10.22) and (10.23) lead to identical results. If the particle absorbs the incident radiation, then the index of refraction is complex, and the efficiency factor of absorption Q_A is obtained from the definition of Q_E (10.18) in the form of

$$Q_A = Q_E - Q_S. \tag{10.24}$$

The efficiency factor for the backscattering cross-section Q_{BS} can be presented as follows:

$$Q_{BS} = \frac{\sigma_{BS}}{\pi a^2} = \frac{1}{x^2}\left|\sum_{n=1}^{\infty}(2n+1)(-1)^n(\dot{a}_n - \dot{b}_n)\right|. \tag{10.25}$$

In radar technology this parameter was called the effective scattering area (ESA) of a target (Skolnik, 1980). In this case the diagram showing the dependence of ESA on the angle of wave incidence on a scatterer is called the ESA diagram (this is just the scattering indicatrix, in its essence).

The complex $\dot{a}_n$ and $\dot{b}_n$ coefficients in formulas (10.22), (10.23) and (10.25) are called the Mie coefficients. They represent complicated functions, expressed in terms of the Riccati–Bessel functions, and are written in the form:

$$\dot{a}_n = \frac{\Psi_n(x)[\Psi_n'(y)/\Psi_n(y)] - \dot{m}\Psi_n'(x)}{\xi_n(x)[\Psi_n'(y)/\Psi_n(y)] - \dot{m}\xi_n'(x)}, \tag{10.26}$$

$$\dot{b}_n = \frac{\dot{m}\Psi_n(x)[\Psi_n'(y)/\Psi_n(y)] - \Psi_n'(x)}{\dot{m}\xi_n(x)[\Psi_n'(y)/\Psi_n(y)] - \xi_n'(x)}, \tag{10.27}$$

where the prime denotes differentiation with respect to the argument under consideration. The Riccati–Bessel functions $\Psi_n(z)$ and $\xi_n(z)$ are associated with the Bessel function of non-integer order by the relations:

$$\Psi_n(z) = \left(\frac{\pi z}{2}\right)^{1/2} J_{n+1/2}(z), \tag{10.28}$$

$$\xi_n(z) = \left(\frac{\pi z}{2}\right)^{1/2} J_{n+1/2}(z) + (-1)^n \mathrm{j} J_{-n-1/2}(z), \tag{10.29}$$

where $z = x$ or y, and the complex argument y is determined as follows $y = \dot{m}x$.

The physical sense of the Mie coefficients is as follows. The primary (external) electromagnetic wave excites some particular forced oscillations inside the substance of a sphere and on its surface. These forced oscillations can be subdivided into the electric and magnetic modes of oscillations on the basis of the existence of a corresponding radial component in a scattered (forced) field. So, if the electric vector of a scattered field has a radial component, which is caused by electric charges distributed over the surface, then such a mode of oscillations is called the oscillations of electrical type. The amplitudes of oscillations of such a type are expressed in terms of b_n coefficients. If the scattered field is excited by means of a_n coefficients only, then the structure of the field will be as if it was produced by variable magnetic charges disposed on the surface of a sphere. And such a field is called a field of magnetic type. Thus, it can be considered (Stratton, 1941), that a_n coefficients represent the amplitudes of oscillations of magnetic type, and b_n coefficients those of electrical type. If the frequency of an impressed (external) field approaches any characteristic frequency of the natural electromagnetic oscillations of a system, then the resonance phenomenon arises. This is just the condition where the denominators in expressions (10.26) and (10.27) tend to zero. But since in a system (inside the sphere) the absorption is always present, the denominators of the Mie coefficients can be reduced to their minimum values, but they cannot be made equal to zero. Thus, the mathematical catastrophe – the arising of infinite amplitudes – does not occur.

Though the Mie solution is strictly applicable to the whole range of $m - x$ values, it was found fairly quickly, that the numerical calculations of a scattering indicatrix and efficiency factors for arbitrary m and x values are rather laborious. For example, the convergence of series determining the Mie coefficients becomes very slow when the relative size of a sphere increases as compared to the incident radiation wavelength. Another difficulty consists in the irregularity of the values of a_n and b_n coefficients. On one hand, this makes the interpolation procedures rather unreliable (Shifrin, 1951, 1968), and, on the other hand, in performing detailed numerical calculations, a lot of resonance modes arise, some of which can be 'false' (Conwell *et al.*, 1984). Fortunately, for many practically important tasks (including remote sensing) there is no necessity to perform calculations by the Mie theory throughout the range of $m - x$ values. One can restrict calculations to the limiting values of the Mie solution, which, in their turn, can be determined by simplified techniques. So, for example, for high values of parameter x (i.e. for a large spherical particle as compared to the wavelength) the convergence of the accurate Mie solution becomes very poor. However, in such cases the geometric optics laws are applicable for determining the scattering indicatrix and efficiency factors, and the final expressions become quite simple. For very small x values the accurate Mie formula is essentially simplified, if one applies the power series expansions of spherical Bessel functions with respect to Mie's a_n and b_n coefficients. However, the procedure of expansion of efficiency factors in power series with respect to small x values and the physical interpretation of expansion terms turns out to be rather complicated.

Detailed investigations of mathematical features of the expressions for efficiency factors, undertaken for a wide frequency band of electromagnetic waves and for dielectric properties of substances encountered in natural media, have shown that three regions can be found in which the scattering on particles possesses some peculiarity.

The first region, or the Rayleigh scattering region, is characterized by the following conditions: first, the size of particles is small as compared to the wavelength of an external field, i.e. $a \ll \lambda (x \ll 1)$; and, second, $|\dot{m}|x \ll 1$. The first condition implies that we are in the quasi-static approximation (see section 1.6) and can make use of the laws of electrostatics. The second condition requires the absence of electromagnetic resonances inside a particle. As usual, the traditional value of $a = 0.05\lambda (x < 0.3)$ is accepted as an upper limit of a particle's radius for this approximation. But in this case the second condition should, certainly, be satisfied as well.

The second region, or the resonance (the Mie) scattering region, is characterized by the presence of a great number of resonance features and very complicated scattering indicatrix. For these reasons this region has proved to be most complicated for investigations. The values of x are usually concluded within the limits of 0.25–0.5 to 50.

The third region (the high-frequency region, or the geometrical optics region) is characterized by the presence of a geometrical shadow behind the particle. This results in the situation where the extinction cross-section will tend to the doubled geometrical cross-section of a particle (of arbitrary shape, it should be added). This

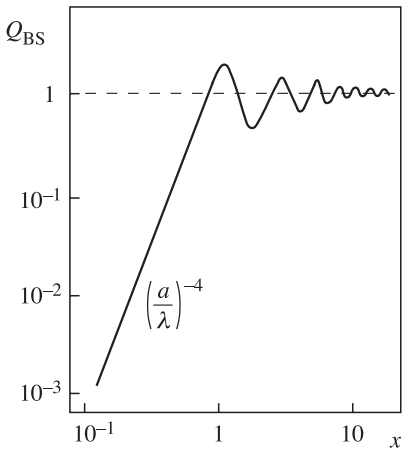

Figure 10.3. The backscattering efficiency factor of a metal sphere as a function of the size parameter (at microwave bands).

phenomenon is called the extinction paradox, and it has several (and different) physical explanations.

As an indicative example, we shall consider the dependence of the efficiency factor of backscattering for a metal sphere (Figure 10.3). This object is often used as an experimental standard for calibrating microwave antenna systems and complicated receiving radio-engineering complexes (early-detection radar stations, for instance).

From the analysis of the plot, presented in the logarithmic scale, it can easily be seen that the whole region of the size parameter values can really be subdivided into three characteristic sub-regions: the Rayleigh scattering region, where Q_{BS} decreases as $1/\lambda^4$; the resonance Mie region, where the resonance dependencies are explicitly exhibited; and the geometrical optics region, where the Q_{BS} value is equal to the geometrical cross-section value of a large particle. Of interest is the fact that for the dimension parameter value equal to unity takes place the first and most strong Mie resonance, at which the backscattering cross-section exceeds by nearly three times the size of the geometrical shadow. Physically, this is due to the fact that the sphere intensively scatters 'backwards' as a resonance half-wave vibrator, i.e. $\pi a = \lambda/2$.

10.3 RAYLEIGH SCATTERING FEATURES

Because the features of electromagnetic field scattering by small particles are of great importance for practical applications (and for remote sensing primarily), we shall consider in more detail the features of Rayleigh scattering.

For small particles ($x \ll 1$), provided that the internal resonances are absent $|\dot{m}|x \ll 1$, the exact Mie formulas are simplified, if we use the power series expansion of spherical Bessel functions with respect to the Mie coefficients. The expansion of

the Mie solution in power series with respect to small x values can be presented as follows (Shifrin, 1951; Hulst, 1981):

$$Q_{\mathrm{E}} = -\mathrm{Im}\left\{4x\frac{m^2-1}{m^2+2} + \frac{4}{15}x^2\left(\frac{m^2-1}{m^2+2}\right)^2\frac{m^4+27m^2+38}{2m^2+3} + \cdots\right\}$$
$$+ \mathrm{Re}\left\{\frac{8}{3}x^4\left(\frac{m^2-1}{m^2+2}\right)^2 + \cdots\right\}. \tag{10.30}$$

Separate investigations have shown that the first term (in braces) characterizes the efficiency factor of absorption, and the second term characterizes the efficiency factor of scattering. The result is valid for $x \ll 1$ and $|\dot{m}|x \ll 1$.

It is quite useful to obtain similar results proceeding from physical approaches. We shall make use of two approaches: we consider the scattering on a small particle in the quasi-static approximation and the scattering on a solitary dipole emitter.

It is known from electrostatics that the field inside a dielectric sphere, placed in the permanent external electric field $\mathbf{E}_{\mathrm{i}}$ with linear polarization, is homogeneous and equals (Stratton, 1941):

$$\mathbf{E} = \frac{3}{\varepsilon+2}\mathbf{E}_{\mathrm{i}};\ \mathbf{E}_{\mathrm{i}} = E_0\mathbf{e}_{\mathrm{i}}, \tag{10.31}$$

where $\mathbf{e}_{\mathrm{i}}$ is the unit vector in the direction of incident wave polarization.

Substituting this relation into (10.15), we obtain the expression for a scattering amplitude for the external field with linear polarization in the form:

$$f(\mathbf{\Omega}', \mathbf{\Omega}) = \frac{k^2}{4\pi}\left[\frac{3(\varepsilon-1)}{\varepsilon+2}\right]V[-\mathbf{\Omega}\times[\mathbf{\Omega}\times\mathbf{e}_{\mathrm{i}}]]. \tag{10.32}$$

Note that the double vector product is here the sine of angle θ_0 between the polarization vector and the direction of observation, and V is the geometrical volume of a particle. The differential scattering cross-section of a particle will be equal, in accordance with (10.6), to

$$\sigma_{\mathrm{d}}(\theta_0) = \frac{\pi^2}{\lambda^4}\left[\frac{3(\varepsilon-1)}{\varepsilon+2}\right]^2 V^2\sin^2\theta_0. \tag{10.33}$$

Note that the scattering cross-section is inversely proportional to the fourth power of wavelength and directly proportional to the square of the volume scatterer's. It was these two properties of small scatterers which were obtained by Rayleigh by bringing in the theory of dimensions.

It is of interest is to compare the relation obtained with the backscattering cross-section. Substituting the value of angle $\theta_0 = (3/2)\pi$ into (10.33) and remembering formula (10.7), we have:

$$\sigma_{\mathrm{BS}} = \frac{4\pi^3}{\lambda^4}\left[\frac{3(\varepsilon-1)}{\varepsilon+2}\right]^2 V^2. \tag{10.34}$$

As would be expected, all basic features of scattering in the Rayleigh region (the wavelength and volume dependencies) have conserved for backscattering as well.

Using relation (10.12), we shall consider now the scattering cross-section for a small dielectric particle:

$$\sigma_S = \iint_{4\pi} \sigma_d \, d\Omega = \frac{\pi^2}{\lambda^4} \left[\frac{3(\varepsilon - 1)}{\varepsilon + 2}\right]^2 \int_0^{\pi} \sin^3 \theta \, d\theta \int_0^{2\pi} d\varphi = \frac{128\pi^5 a^6}{3\lambda^4} \left(\frac{\varepsilon - 1}{\varepsilon + 2}\right)^2. \quad (10.35)$$

Separating this expression with the real geometrical cross-section, we obtain the well-known Rayleigh equation (or relation) for the efficiency factor of scattering (with allowance for the size parameter of a particle):

$$Q_S = \frac{8}{3} x^4 \left(\frac{\varepsilon - 1}{\varepsilon + 2}\right)^2. \quad (10.36)$$

Comparing the obtained expression with the expansion of the accurate Mie solution (10.30), we see that the Rayleigh approximation is a direct consequence of the Mie solution (the first term in the real part of the expansion) for purely dielectric spheres. The absorption cross-section is zero in this case (see relation (10.16)). Using the obtained expressions (10.33) and (10.35), we shall obtain the expression for the indicatrix of scattering of linearly polarized radiation by a small particle:

$$p(\theta_0) = 4\pi \frac{\sigma_d}{\sigma_s} = \frac{3}{2} \sin^2 \theta_0. \quad (10.37)$$

It follows from this expression that for small particles there takes place a very strong and peculiar feature in the angular characteristics of scattering – the scattering indicatrix has the form of a torus; in this case the maximum of scattering is observed in the direction of reverse and direct scattering ($p = 3/2$). In the directions with $\theta_0 = 0$ and 180° the scattering is completely absent. This feature of Rayleigh scattering is often used for interpreting physical and observational experiments with coherent sources.

Another physical approach is related to using the features of the radiation (i.e. considered in the far zone) field of an elementary emitter in electrodynamics: the dipole – which can be excited by the external electromagnetic field. The radiation field of a dipole is known (Born and Wolf, 1999) to consist of one electric component E_θ and one magnetic component H_φ, the vectors being in phase. The electric component is related with its polarization vector **P** as follows:

$$E_\theta = k^2 |\dot{P}| \frac{\exp(\mathrm{j}kR)}{R} \sin \theta, \quad (10.38)$$

where θ is the polar angle measured from the direction of the polarization vector. In its turn, the polarization vector is related with the complex polarizability α and the external field as $\dot{P} = \dot{\alpha} E_i$. By the polarizability of particles is meant their capability to acquire the dipole moment in the external electric field. For relatively simple physical systems the relationship between the polarizability α and macroscopic dielectric properties of substance can be established by means of the Lorentz – Lorenz

formulas (Prochorov, 1984):

$$\dot{\alpha} = \frac{\dot{\varepsilon} - 1}{\dot{\varepsilon} + 2} \frac{3}{4\pi} V. \tag{10.39}$$

Substituting expression (10.38) into (10.6), we obtain the value of the scattering amplitude for the dipole:

$$\dot{f}(\theta) = k^2 \dot{\alpha} \sin\theta. \tag{10.40}$$

Making computational procedures similar to those presented above, we shall obtain for the efficiency factor exactly the same expression as (10.36). For these reasons Rayleigh scattering is sometimes called dipole-type scattering.

The absorption cross-section can be obtained from expression (10.16), if we substitute into it relation (10.31), in the form of

$$\sigma_A = k\varepsilon_2 \left| \frac{3}{\dot{\varepsilon} + 2} \right|^2 V. \tag{10.41}$$

And then for the efficiency factor of absorption we shall have:

$$Q_A = \frac{4}{3} x\varepsilon_2 \left| \frac{3}{\dot{\varepsilon} + 2} \right|^2 = 12x \frac{\varepsilon_2}{|\dot{\varepsilon} + 2|^2}. \tag{10.42}$$

The expression obtained exactly corresponds to the first term in the imaginary part of the expansion of the accurate Mie solution (10.30).

It is important to consider some special cases, which are often met with in observational practice.

10.3.1 Metal particles

The dielectric properties in the microwave band of such substances are characterized by high values of real and imaginary parts of the dielectric constant. It follows from this circumstance, that $Q_S \approx (8/3)x^4$, and $Q_A \to 0$. In other words, small metal particles intensively scatter electromagnetic radiation and, virtually, do not absorb it.

10.3.2 Soft particles

By such kind of particles are meant the particles, whose substance possesses very weak absorbing properties ($\varepsilon_2 \ll 1$) (transparent particles) and whose index of refraction is close to unity $(\varepsilon_1 - 1) \ll 1$. Such particles include water particles in the optical band, aerosol particles in the atmosphere in the microwave band and many other types of particles. It follows from this fact that $Q_S \approx (8/3)x^4(\varepsilon_1 - 1)^2$, and $Q_A \approx (4/3)x\varepsilon_2$. Unlike with metal particles, the general picture of scattering of soft particles will radically change depending on the relationship between the size and properties of the particles' substance. For very small particles ($x < 0.05$) the albedo can be approximated as follows: $\omega \sim 10^3 x^3$, and, thus, as the size of particles decreases, their absorbing properties will essentially prevail over scattering ones, in spite of a very weak absorption of the particles' substance itself. Figure 10.4 presents

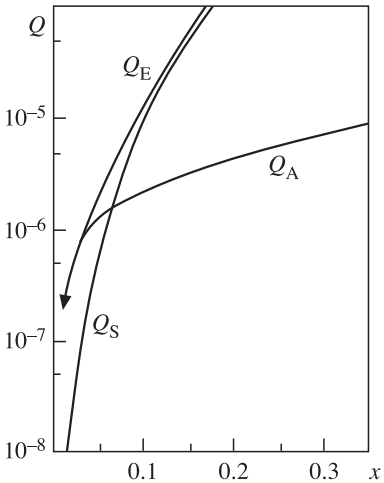

Figure 10.4. The efficiency factors of scattering (Q_S), absorption (Q_A) and extinction (Q_E) for small spheres (in the case of light loss, $m = 1.32 - j10^{-5}$) as a function of the size parameter (Deirmendjian, 1969).

the calculated values of the factors of efficiency of extinction, scattering and absorption for small, but finite-in-size dielectric spheres ($0.025 < x < 0.35$) with weak absorption. The analysis of this figure indicates that for such particles the critical size, in a certain sense, will be of the order of 0.05–0.1. When this size is exceeded, the particles become purely scattering ($\omega \to 1$), as a matter of fact.

10.3.3 Water particles

As we have noted (Chapter 8), the dielectric characteristics of water possess prominent frequency properties in the microwave band. For these reasons the general picture of the scattering of water particles will essentially change depending on the relationship between the physical size of particles and the working wavelength band. Nevertheless, some estimations of the behaviour of scattering and absorption factors can be made now. So, for centimetre and decimetre bands for fresh water (see Chapter 8) $\varepsilon_1 \gg 1$ and $\varepsilon_2 < 1$, and, thus, $Q_S \approx (8/3)x^4$ and $Q_A \approx 12x\,\mathrm{tg}\delta(1/\varepsilon_1)$. For small particles ($x < 0.05$) the albedo can be approximated as follows: $\omega \sim 3 \times 10^3 x^3$, and, thus, as the particle size decreases, the absorbing properties of water drops will essentially prevail over scattering ones, as in the case of soft particles.

In conclusion to this section, we summarize the Rayleigh scattering features as follows:

- the scattering cross-section (and backscattering cross-section) is inversely proportional to the fourth power of the wavelength and directly proportional to the square of the scatterer's volume;

- the absorption cross-section is inversely proportional to the first power of the wavelength and directly proportional to the value of the scatterer's volume;
- the scattering has dipole character and does not depend on the shape of particles;
- the scattering indicatrix for the wave of linear polarization has toroidal shape of the surface; in this case the scattering maximum is observed in the direction of reverse and direct scattering ($p = 3/2$). In the directions with $\theta_0 = 0$ and 180° the scattering is absent altogether. For non-polarized radiation the indicatrix can be presented in the form of

$$p(\theta_0) = \frac{3}{4}(1 + \cos^2 \theta_0). \tag{10.43}$$

The indicated features of scattering are rather peculiar and are not met in the other scattering regions (the Mie region and the geometrical optics region). For this reason they are often used in observational practice as characteristic signs for the detection of Rayleigh-type scattering.

10.4 FEATURES OF SCATTERING PROPERTIES OF AQUEOUS PARTICLES

The most important class of scatterers in the terrestrial atmosphere are aqueous drops, which are present in various physical media, such as cloudy systems of various classes, fogs, precipitations of various types, and spray sheet on a stormy sea surface.

As we noted earlier (Chapter 8), the dielectric characteristics of water possess prominent frequency features in the microwave band. For these reasons the general picture of scattering of aqueous particles will essentially change depending on the relationship between the physical size of particles and the working wavelength band, and in each particular case of experimental investigations the detailed calculation of scattering parameters is required. It is necessary to make use of the available calculation tables for the microwave band with subsequent interpolation procedures (Krasiuk and Rosenberg, 1970; Skolnik, 1980; Oguchi, 1983; Lhermitte, 1988; Bohren and Hoffman, 1983; Ivazyn, 1991). Nevertheless, we shall demonstrate, for a series of examples, some general properties of electromagnetic waves scattering by aqueous spheres.

Figure 10.5 presents calculated values of efficiency factors of extinction, scattering and backscattering for aqueous spheres at wavelengths of 0.8 and 0.2 cm depending on the size parameter in the range of its values up to 15. Considering the plots of the region of values for $x < 1$, it can easily be seen that the behaviour of efficiency factors corresponds to the features of the Rayleigh region (see section 10.3). The prominent maximum is observed in the Mie region for all efficiency factors at $x = 1$. However, as the size parameter increases, the extinction and scattering decrease very slowly to the values equal to two and unity, respectively, not exhibiting any prominent resonance properties in this case. Unlike extinction and

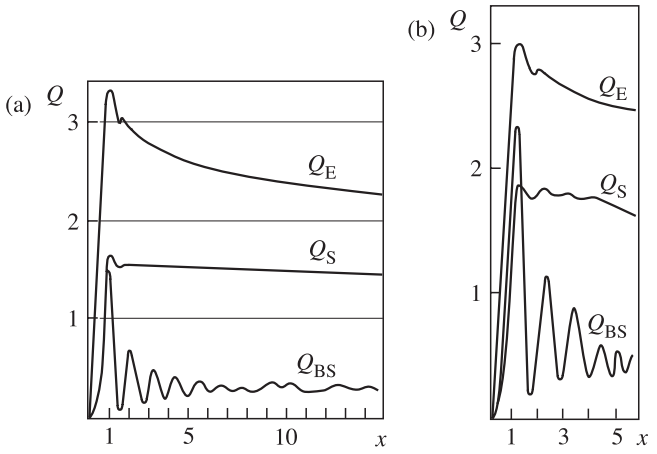

Figure 10.5. The efficiency factors of scattering (Q_S), backscattering (Q_{BS}) and extinction (Q_E) for aqueous spheres: (a) $\lambda = 0.2$ cm and $t = 20°C$; (b) at $\lambda = 0.8$ cm and $t = 20°C$.

total scattering, the backscattering possesses sharp and strong resonance properties up to the values of $x = 10$. In the geometrical approximation the efficiency factor of extinction becomes equal to two, i.e. it twice exceeds the geometrical diametre of a sphere ('the extinction paradox'). In this case the rate of tending to their limiting values is essentially different for extinction and for scattering; as a result, for large drops the losses for scattering exceed the losses for absorption. This circumstance is well illustrated by the calculated plot (in the bilogarithmic scale) of a single scattering albedo that depends on the size parameter of spheres (Figure 10.6). The data were calculated in a wide range of frequencies – from 4 GHz (the wavelength of 7.5 cm) up to 100 GHz (the wavelength of 3 mm) – and of drops' radii (0.5–3.0 mm). Virtually irrespective of the wavelength band, for $x < 0.5$ the albedo is lower than 0.1, and the scattering contribution to the total losses is very small. Note that in this case the decrease of albedo for small drops has a prominent character of exponential dependence as x^3, as it should be expected for the Rayleigh region (see section 10.3). For $x > 1$ the contribution of scattering into the total losses of large drops sharply increases, reaching 60–70% of the total losses (in other words, of the extinction).

Figure 10.7 presents the frequency dependencies (in the bilogarithmic scale) of the efficiency factor of extinction for aqueous spheres with fixed radii in a wide frequency band – from 5 GHz (6 cm) to 300 GHz (1 mm). The analysis of this figure shows all the aforementioned characteristic regions of scattering – for large wavelengths the exponential drop as λ^{-n} is observed for the sphere of fixed radius. This dependence characterizes the beginning of the Rayleigh scattering region. For short wavelengths the efficiency factor of extinction tends to the value of 2. At intermediate wavelengths the resonance Mie maximum is observed (it is rather smeared in this coordinate system). It is interesting to note that the plot clearly demonstrates only the transition region from the first Mie maximum to the Rayleigh region and the very beginning of the Rayleigh region. So, as the fixed

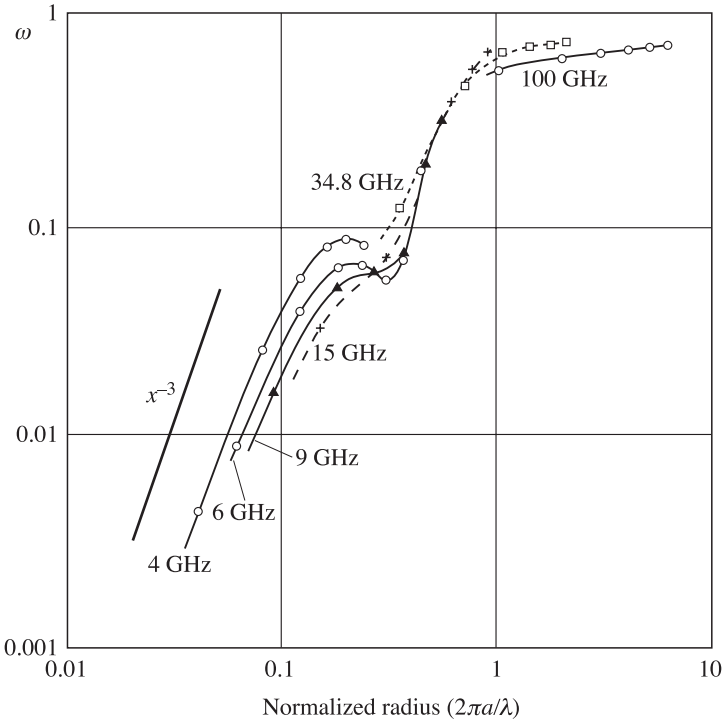

Figure 10.6. Single-scattering albedo of aqueous spheres as a function of size parameter (normalized radius) at 4, 6, 9, 15, 34.8 and 100 GHz. The points on each curve correspond from the left, to drop radii 0.5, 1.0, 1.5, 2.0, 2.5 and 3.0 mm respectively (Oguchi, 1983).

radius decreases, the exponent of the power-law drop also decreases and finally reaches a value equal to two, but already in the purely Rayleigh region (see (10.30)).

10.5 ELECTROMAGNETIC PROPERTIES OF POLYDISPERSE MEDIA

As we have already noted (section 1.6), the structure of a substance in the Maxwell theory is specified by introducing the phenomenological dielectric and magnetic parameters for continua. In radiative transfer theory (the macroscopic version) the structure of a substance is presented in a different manner – in the form of a cloud of randomly distributed particles in a continuum (for example, in the terrestrial atmosphere or in the sea) with the parameters of attenuation and scattering in a medium (calculated per unit of a beam path in a medium). A lot of quite various physical structures in the terrestrial atmosphere and in the ocean can be attributed to such kinds of media. Virtually all of them have the character of polydisperse media, i.e. media with particles of different sizes. Physically, this is related with the circumstance that, because all polydisperse media are open physical systems, a certain dynamical

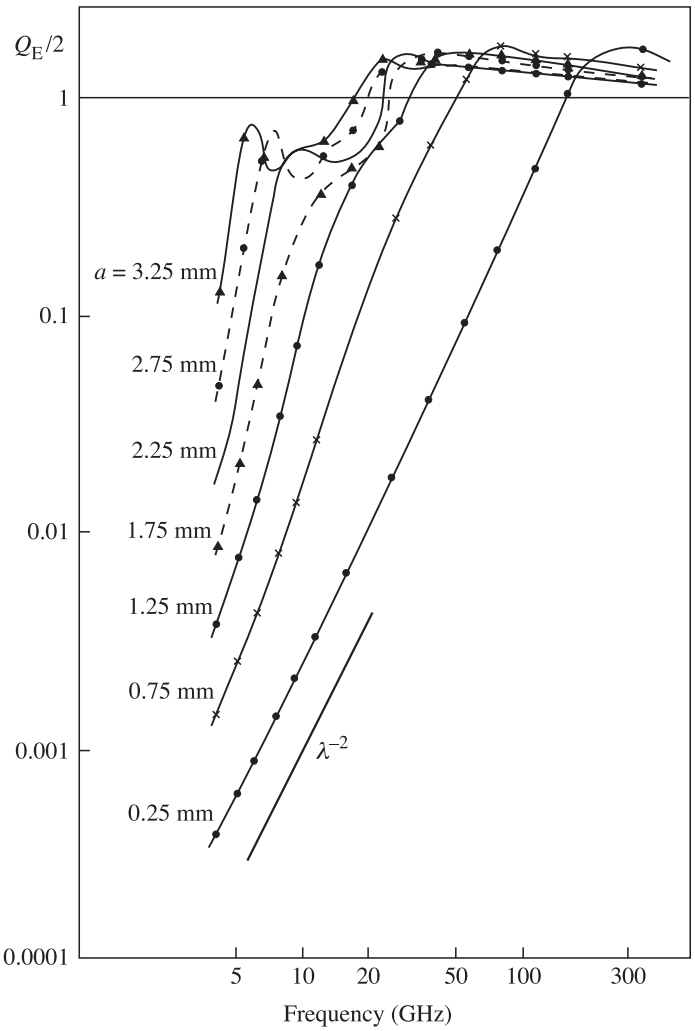

Figure 10.7. The extinction factor of spherical raindrops as a function of frequency ($t = 20^{\circ}$C) (Oguchi, 1983).

equilibrium can be established in the dynamical process of particles' birth and death only. The latter circumstance stipulates the principal presence of polydisperse-composed particles in media. In this section we shall consider the basic mechanical characteristics which are used in describing the disperse mixtures, and the procedure of transition from the characteristics of scattering of individual particles to the electromagnetic parameters of a unit volume.

Physical systems consisting of some combination of substances (which are, by themselves, in different phase states) are usually subdivided into two large classes: heterogeneous mixtures and homogeneous mixtures (Nigmatulin, 1978).

By heterogeneous mixtures here are meant systems which contain macroscopic (with respect to molecular scales) and chemically non-interacting inhomogeneities (or admixtures). From a huge number of possible heterogeneous mixtures existing in nature, some comparatively regular structures can be distinguished which are called disperse mixtures. Such systems, which usually consist of two phases, include, for example, aqueous drops in air or air bubbles in sea water (the so-called aerated layer) and the hexagonal structure in sea foam. In this case the particles are called a disperse phase, and their carrier medium the disperse phase. By *homogeneous mixtures* are meant systems in which the substance is intermixed at the molecular level. The so-called *colloidal mixtures* occupy an intermediate position.

Below we shall consider some mechanical characteristics determining the dispersity of disperse systems.

10.5.1 The density function

The most important characteristic of the microstructure (dispersity) of disperse systems is the differential density function of particles in size, designated by $n(r, x, y, z, t)$, where r is the radius of particles (instead of the radius, sometimes the diameter, surface, volume or mass of particles are used); x, y, z are spatial coordinates; t is time. Proceeding from the definition, quantity $n(r, x, y, z, t)\,\mathrm{d}r\,\mathrm{d}x\,\mathrm{d}y\,\mathrm{d}z$ is the number of particles having radius from r to $r + \mathrm{d}r$ in the volume of $\mathrm{d}x\,\mathrm{d}y\,\mathrm{d}z$ in the vicinity of point (x, y, z) at time instant t. Naturally, in the practice it is impossible to determine the value of $n(r, x, y, z, t)$ at all points of the studied space simultaneously. For this reason the microstructure of a disperse system is often characterized by *size spectra* of particles $n(r)$, averaged over time and space, or by related integral distribution parameters, which are proportional to distribution moments of any order. For example, the important characteristics of a disperse medium's microstructure are the density of particles, the total mass of water (or water content) and the radar reflectivity.

In the theoretical respect the density function plays a fundamental part, since it determines the physical features of a system and its possible evolution.

It follows from physical considerations that for $r \to 0$ and for $r \to \infty$ the density of a number of particles must tend to zero (within the framework of the given physical system). The dimension of this parameter, as can easily be seen from its definition, in cm^{-4}.

10.5.2 The volume density of particles

An important integral parameter is the volume density of particles (or the number density) N (cm^{-3}), defined by the following integral transformation from the spectrum of particles:

$$N(\mathrm{cm}^{-3}) = \int_0^\infty n(r)\,\mathrm{d}r = \int_0^\infty n(D)\,\mathrm{d}D, \tag{10.44}$$

where D is the diameter of particles. This characteristic determines the absolute number of particles in a unit volume. It follows from this relation, that $n(r) = 2n(D)$.

10.5.3 The integral distribution function

In experimental practice it is often convenient to present the observational results in the form of volume density of particles with the lower variable limit $N(r)(\mathrm{cm}^{-3})$, i.e. in the form:

$$N(r) = \int_r^\infty n(r)\,\mathrm{d}r. \tag{10.45}$$

This characteristic determines the absolute number of particles in a unit volume beginning with some particular (fixed) value of size. A lot of measuring devices, which record the size of particles, operate using this particular characteristic, and in order to transfer to the density function it is necessary to perform numerical (or graphical) differentiation of obtained results.

10.5.4 The relative density function

In theoretical analysis, as well as in processing and comparing the experimental results of various types, it is expedient to use the relative density distribution function in the form:

$$f(r) = \frac{n(r)}{N}; \int_0^\infty f(r)\,\mathrm{d}r = 1. \tag{10.46}$$

As can be seen from the definition, the dimension of this parameter is cm^{-1}.

10.5.5 The density sampling probability

In the experimental respect, the dispersity characteristics of a system are usually found by detecting and estimating the density sampling probability, or, in other words, by forming and constructing experimental histograms. This procedure is rather complicated, in general, and requires from a researcher both experience and skills in solving such tasks, and a clear understanding of the basic physical problem. We shall briefly describe this procedure, predominantly in the qualitative respect.

Let the experimental data on particles obtained range in radius from a to b. The total number of recorded particles is N. We divide the range of radii by j, the number of bunching intervals. In each of these intervals N_j particles will be recorded. The size of a bunching interval equals Δr_j. Then by

$$P_j = \frac{N_j}{N}; j = 1, \ldots, k \tag{10.47}$$

will be meant a sampling probability of the presence of particles in the given bunching interval. Here k is the total number of bunching intervals. Here

$$N = \sum_{j=1}^{k} N_j. \tag{10.48}$$

The sampling probability $P_j(r_j)$, presented in graphical form, represents the experimental histogram.

By the density function of sampling probability is understood the following quantity:

$$f_j(r_j) = \frac{N_j}{N\left(\frac{b-a}{k}\right)}. \tag{10.49}$$

From the normalization conditions it follows that

$$\sum_{j=1}^{k} f_j(r_j)\,\Delta r_j = 1. \tag{10.50}$$

If the sizes of bunching intervals are the same (Δr), then the relationship between the density function of the sampling probability and the sampling probability (the experimental histogram data) can be presented as follows:

$$f_j(r_j) = \frac{P_j}{\Delta r}(\mathrm{cm}^{-1}). \tag{10.51}$$

It can easily be concluded from the relation obtained, that $f(r_j)$ is the finite-difference analogue of the relative distribution function (10.46).

10.5.6 The total mass and the relative volume concentration of water

In some meteorological problems, as well as in the tasks of microwave sensing of the terrestrial atmosphere, it is necessary to know the total mass of a substance (the water, for example) in a unit of volume of the disperse medium (the cloud, for example). If the disperse medium consists of regular spheres of various diametre, then, by definition, the total mass of substance in a unit volume (or the water weight content, conventionally) W (g/cm^3) can be obtained from the following relation:

$$W = \frac{4}{3}\pi\rho\int_0^\infty r^3 n(r)\,\mathrm{d}r = \frac{4}{3}\pi\rho N\int_0^\infty f(r) r^3 \mathrm{d}r, \tag{10.52}$$

where r is the density of substance of spheres.

In many application problems it is necessary to know the relative volume concentration of substance (or volume concentration), C (the dimensionless quantity), which can be obtained from the following relation:

$$C = \frac{W}{\rho} = \frac{4}{3}\pi\int_0^\infty r^3 n(r)\,\mathrm{d}r. \tag{10.53}$$

The characteristics considered are proportional to the third moment of the size distribution of particles. However, some remote investigations, such as radar studies of the structure of cloudy systems, require knowledge of the moments of much higher order.

10.5.7 Radar reflectivity

By this characteristic $Z(\mathrm{cm}^3)$ is meant the following quantity:

$$Z = \int_0^\infty n(r) r^6 \, \mathrm{d}r. \tag{10.54}$$

The physical sense of this characteristic can easily be understood using the expression for backscattering of an individual particle (10.34) in the Rayleigh approximation in calculating the backscattering of a unit volume σ_0 with the density function of reflective spheres $n(r)$:

$$\sigma_0 = \int_0^\infty \sigma_{\mathrm{BS}} n(r) \, \mathrm{d}r = \frac{64}{\lambda^4} \pi^5 \left| \frac{\dot{\varepsilon} - 1}{\dot{\varepsilon} + 2} \right|^2 \int_0^\infty n(r) r^6 \, \mathrm{d}r \tag{10.55}$$

This relation indicates that the signal, scattered back from a cloudy structure, is proportional to the sixth moment of the density function of drops in a cloudy mass. It can easily be seen from this result that drops of large and super-large size (having $r > 100$ micrometre) play a very essential part in the process of backscattering electromagnetic radiation from cloudy systems. Moreover, these drops are main carriers of radar remote information in the cloudy systems (Doviak and Zrnić, 1984; Doviak and Lee, 1985). However, in radiothermal investigations the situation is essentially different – the thermal radiation depends on the total mass of water in a drop cloud and, thus, the signal is proportional to the third moment of the density function of drops in a cloudy mass. All these features are important in the interpretation of observational data.

10.5.8 Rainfall rates

If disperse systems possess prominent dynamical properties (for example, precipitations of various phase types), then in their remote analysis the parameter characterizing the quantity of a substance precipitated on a unit area per unit time is of importance. Such a characteristic, which is widely used in meteorological and remote investigations, is called the rainfall rate, R (cm/s). It is determined by the following expression:

$$R = \int_0^\infty n(r) V(r) \frac{4}{3} \pi r^3 \, \mathrm{d}r, \tag{10.56}$$

where $V(r)$ is the velocity of motion of drops of corresponding radius. For the conditions of rainfall drops in the terrestrial atmosphere a series of empirical relations was established between the precipitation rate and the radius of a drop. They include, in particular, the linear relation $V\ (\mathrm{m/s}) = 75r$ (cm) for sufficiently small-sized rainfall drops, and for larger drops the precipitation rate becomes constant and does not depend on their size (Kollias *et al.*, 1999). This indicates that the rainfall rates will be proportional to the fourth moment (or to the third moment, depending on the diameter of drops) of the density function of drops in a

cloudy mass of precipitating drops. In meteorological practice the dimension of R is usually reduced to millimetres per hour.

10.5.9 Natural polydisperse media

In order to present a generalized qualitative picture of density functions for natural polydisperse systems (for terrestrial atmosphere conditions), we shall consider the data of Figure 10.8. It follows from the analysis of these data that the most finely disperse and, at the same time, most intensive (in density function value) are various types of fogs, i.e. the media which are formed immediately after the phase transition of water vapour into the liquid state. The greatest range in dispersity is occupied by various types of aerosols in the terrestrial atmosphere. In spite of the fact that the aerosol mass constitutes only 10^{-9} of the total mass of the atmosphere, it essentially influences the atmospheric radiation processes and, therefore, the weather and climate as well. Depending on their physicochemical origin, the aerosols are subdivided into five model types: maritime, continental, urban–industrial, volcanic and

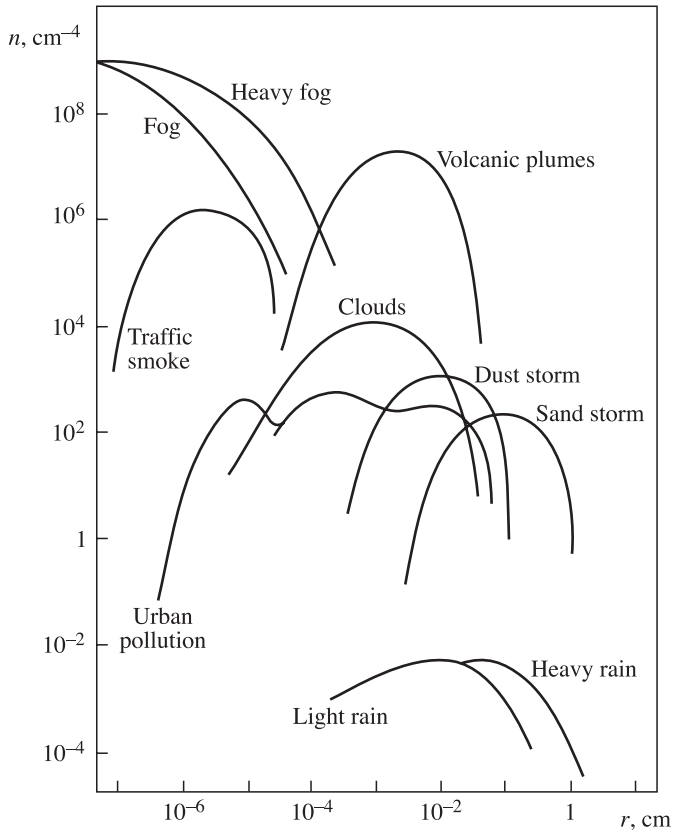

Figure 10.8. Particle-size distributions (the density functions) for natural disperse media.

stratospheric. All these types strongly differ both in the characteristic range of particle size, and in their intensity. The distributions can also have a multimodal form, as in the case of urban aerosol, for instance (Figure 10.8).

The drop-cloudy systems of the terrestrial atmosphere represent an extremely inhomogeneous medium permanently varying in space and in time. This is due, first of all, to the great diversity of particular physical causes and mechanisms of initiating the phase transition of water vapour into the liquid state. Therefore, depending on the spatial–temporal scale of a particular investigation, the distribution parameters can have very wide ranges of variation of their numerical parameters (Deirmendjian, 1969; Ivazyn, 1991; Krasiuk and Rosenberg, 1970; Marchuk *et al.*, 1986; Rozenberg, 1972; Houze, 1993; Marshak *et al.*, 1994; Jameson *et al.*, 1998).

The most grossly disperse systems in the terrestrial atmosphere are meteorological systems with precipitation. As in the case of cloudy systems, precipitations possess strong spatial–temporal variations (the so-called multi-fractal structure) (see Chapter 2). This greatly complicates the interpretation and comparison of remotely sensed and in situ results by the researchers (Rodgers and Adler, 1981; Atlas *et al.*, 1981; Velden and Smith, 1983; Jameson, 1991; Niemczynowicz and Bengtsson, 1996; Olsson, 1996; Kostinski and Jameson, 1997; Taylor and English, 1995; Marshak *et al.*, 1997; Smith *et al.*, 1998; Skofronick-Jackson and Wang, 2000; Simpson *et al.*, 1988, 2000; Deeter and Evans, 2000; Liu and Curry, 2000; Bennartz and Petty, 2001; Lohnert and Crewell, 2003).

10.5.10 Analytical forms of the density function

In the last 50 years a great amount of experimental work has been carried out devoted to searching for the most acceptable analytical form of a density function for disperse systems of various physical natures. From the theoretical side the efforts were directed towards the solution of complicated problems of kinetics of physicochemical media using, for example, the solution of a system of the Fokker–Planck–Smolukhovsky equations. The following analytical expression for the density function, known as the gamma distribution, is considered the most theoretically substantiated one:

$$n(r) = ar^{\mu} \exp(-br^{\gamma}), \tag{10.57}$$

where a, b, μ, γ are the parameters determining all the characteristic features of the distribution. Almost all empirical distributions, formed earlier from the experimental data, can be obtained from the given distribution.

Using expressions (10.44), (10.53) and (10.57), we obtain the following formulas for the relative density:

$$C = \frac{4\pi}{3} \int n(r) r^3 \, \mathrm{d}r = \frac{4}{3} \pi a \gamma^{-1} b^{-(\mu+4)/\gamma} \Gamma\left(\frac{\mu+4}{\gamma}\right). \tag{10.58}$$

Letting $\gamma = 1$, we obtain the expression for the volume density:

$$N = \int_0^{\infty} n(r) \, \mathrm{d}r = ab^{1-\mu} \Gamma(\mu + 1). \tag{10.59}$$

Here, as in (10.58), $\Gamma(x)$ denotes the gamma function (Gradshteyn and Ryzhik, 2000), from which this distribution assumed its name.

Using (10.57) and (10.59), we can obtain the expression for the relative density function:

$$f(r) = b^{\mu-1}\frac{r^{\mu}}{\Gamma(\mu+1)}\exp(-br). \tag{10.60}$$

This distribution is now characterized by two parameters only b and μ. This expression is often written down in a slightly different (but equivalent) form:

$$f(r) = \frac{1}{\Gamma(\mu+1)}\mu^{\mu+1}\frac{r^{\mu}}{r_{\mathrm{m}}^{\mu+1}}\exp\left\{-\mu\frac{r}{r_{\mathrm{m}}}\right\}. \tag{10.61}$$

Here parameter μ characterizes the distribution halfwidth, and parameter r_{m} determines the so-called modal (most probable) distribution radius. Serious efforts are now undertaken to determine these parameters for natural disperse media from the experiment. So, for fogs and clouds the values of parameter μ are concluded within the limits of 1–10, and those of the modal radius within the limits of 0.1–10 micrometres.

It is interesting to mention that in 1948 J. Marshall and W. Palmer suggested a simple empirical relation for the density function of rainfalls in the form:

$$n(r) = N_0\exp(-\Lambda r), \tag{10.62}$$

where

$$N_0 = 1.6\times10^4(\mathrm{m}^{-3}\times\mathrm{mm}^{-1});\ \Lambda = 8.2R^{-0.21}(\mathrm{mm}^{-1}). \tag{10.63}$$

Here radius is expressed in millimetres and R in millimetres per hour.

Such a distribution was found to successfully describe the averaged experimental data both for drizzling rains, for widespread rains, and for convection and thunderstorm rains (true, with significant modification of the numerical values of N_0 and Λ). The Marshall–Palmer drop-size distribution, as well as the distributions close to it (such as the Laws–Parsons relation), are widely used now as well (Oguchi, 1983). One has also managed to obtain a fairly simple empirical relation between precipitation intensity and water content (the mass of substance in a unit volume) in a medium, namely:

$$W = 0.06R^{0.88}, \tag{10.64}$$

where the water content has dimension of grams per cubic metre, and the precipitation intensity millimetres per hour. There exist also other numerical versions of the given formula.

Theoretical and numerical investigations of the physicochemical kinetics problems, including the processes of condensation of water vapour, the coalescence between drops and drop break-up, have shown that, generally, the theoretical spectra of drops are qualitatively close to the exponential Marshall–Palmer distribution, though there are some features, which are not described by a rule of thumb of the given distribution. This relates, first of all, to the multimodal character of theoretical distributions and to considerably greater density in the small drop-size range ($r < 0.1$ mm), than in the case of exponential approximation. All these features result

in noticeable variations in the electromagnetic properties of a medium (Jameson, 1991; List, 1988).

10.5.11 Parameters of attenuation and scattering of a polydisperse medium

In accordance with the basic concept of the radiative transfer theory, namely, the electromagnetic rarefaction of a medium, the incident radiation, falling on an investigated volume from outside, completely 'illuminates' all particles present in a unit volume (see Chapter 9). Therefore, when the medium contains a cloud of spherical particles of the same composition, but of different size, the spectral coefficients of attenuation (extinction) and of scattering can be calculated by formulas

$$\gamma(\mathrm{cm}^{-1}) = \int_0^\infty Q_\mathrm{E} \pi r^2 n(r)\,\mathrm{d}r, \tag{10.65}$$

$$\sigma(\mathrm{cm}^{-1}) = \int_0^\infty Q_\mathrm{S} \pi r^2 n(r)\,\mathrm{d}r. \tag{10.66}$$

When the radiation beam propagates in a medium, which contains N spherical particles of the same composition and the same size (each having radius R) in the unit volume, the cross-sections of absorption and scattering (or the efficiency factors of extinction Q_E and of scattering Q_S) can be related to spectral coefficients of total attenuation (extinction) and scattering by simpler relations:

$$\gamma(\mathrm{cm}^{-1}) = Q_\mathrm{E} \pi r^2 N \tag{10.67}$$

and

$$\sigma(\mathrm{cm}^{-1}) = Q_\mathrm{S} \pi r^2 N. \tag{10.68}$$

If the particles are grouped together in size into the intervals with radius r_j ($j = 1, 2, \ldots, M$), then the integrals presented above can be replaced by the sums. If in expressions (10.65)–(10.66) the integrals cannot be obtained analytically, then numerical integration is carried out and the tables are compiled (Krasiuk and Rosenberg, 1970; Skolnik, 1980; Oguchi, 1983; Lhermitte, 1988; Ivazyn, 1991). It should be emphasized once again that all these expressions are obtained under important physical limitations: the electromagnetic rarefaction of a medium and the absence of interactions between particles.

Consider at first the Rayleigh approximation. Since the absorbing properties of particles prevail in this approximation, the spectral absorption coefficient can be presented as:

$$\gamma = k_1(\lambda) \int_0^\infty r^3 n(r)\,\mathrm{d}r, \tag{10.69}$$

where $k_1(\lambda)$ is the numerical coefficient. On the other hand, the total mass of medium's substance W (in a unit volume) will be equal to

$$W = \frac{4}{3}\pi\rho \int_0^\infty r^3 n(r)\,\mathrm{d}r. \tag{10.70}$$

The comparison of these expressions indicates that the spectral extinction coefficient for a medium with particles in the Rayleigh approximation is proportional to the total mass of substance in a unit volume:

$$\gamma = k_2(\lambda) W \tag{10.71}$$

and, what is very important, it does not depend on the form of the density function. Thus, in remote investigations in the Rayleigh region, information on the form of a density function of the disperse medium cannot be obtained, at least directly.

Since water possesses prominent spectral properties in the centimetre and millimetre bands, for the band of 0.5–10 cm and for liquid-drop clouds ($t = 180^{\circ}\mathrm{C}$) the following simple approximation can be established:

$$\frac{\gamma}{W} = \frac{0,43}{\lambda^2}. \tag{10.72}$$

Here W is expressed in grams per cubic metre and absorption in decibels per kilometre. Physically this is related to the fact that the parameter in expression (10.42), which depends on the dielectric properties of water, has an approximation of type $1/\lambda$ on the long-wavelength branch of the Debye relaxation maximum (see Chapter 8). However, in the case of crystalline clouds (hailstones, snowflakes) the extinction decreases by two to three orders of magnitude (other things being equal). And the wavelength dependence can be accepted to be $1/\lambda$ (because the explicit wavelength dependence of the real part of the dielectric constant is absent for ice). There also exist some further experimental data approximations in the Rayleigh region. However, all of them have a frequency character close to (10.72).

Consideration of a wider range of particle size and wavelength requires numerical operations with (10.65) and (10.66). Special calculations of the coefficient of extinction per unit of path (the specific attenuation – attenuation for a 1-km propagation path), carried out in the 1–1000 GHz range for various drop-size distributions and precipitation intensities (Figure 10.9), have shown that the frequency dependencies have a characteristic form – a rapidly growing rise from the side of large wavelengths, a weak maximum in the frequency range of about 100 GHz and a slow drop to the side of higher frequencies. As would be expected, these dependencies do not reveal any sharp maxima which are specific for the Mie region of an individual particle. Besides, the growing regions can be characterized as transition regions from the 'smeared' Mie maximum to the Rayleigh region. In this case the frequency approximation of extinction for high-intensity precipitation, which has large-sized drops and, accordingly, a great scattering, is closer to the $1/\lambda^4$ dependence. Whereas for weak precipitation (with a small dispersity of drops and, accordingly, with very weak scattering and strong absorption, this approximation is closer to that of the Rayleigh region – $1/\lambda^2$ (see relation (10.72) and Figure 10.9). It should also be noted that the distinctions in extinction values for various distributions are the greater, the higher the working frequency and the lower the precipitation intensity. We have already said that the Rayleigh region is not sensitive to the form of distribution of drops (see expression (10.71)). As to the strong precipitations, in this case the intensive scattering of large-sized drops in some sense 'blocks' the

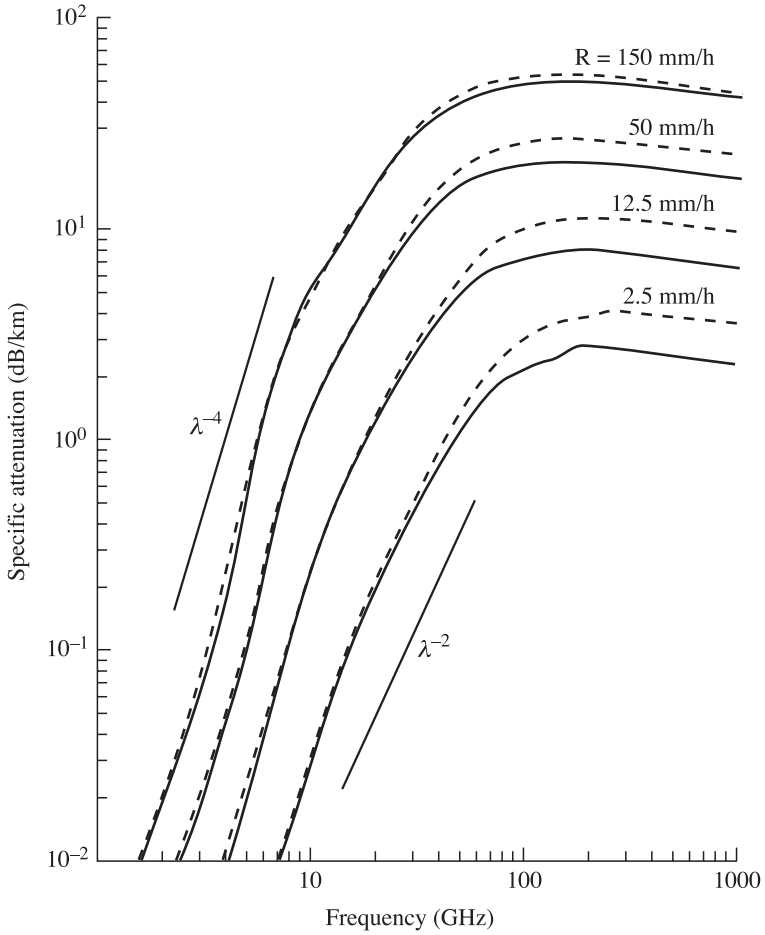

Figure 10.9. Frequency characteristics of rain attenuation at rain temperature of 20°C, for Laws–Parsons (solid curves) and Marshall–Palmer (dashed curves) drop-size distributions. Parameters are rain rates (mm/h) (Oguchi, 1983).

contribution from the absorption of small-sized drops into the total extinction of a disperse medium. Special experiments (Oguchi, 1983; Wolf and Zwiesler, 1996) have really shown that in the millimetre frequency band for rainfalls in the terrestrial atmosphere the sensitivity of the degree of extinction in a medium to the type of distribution is very high, and, therefore, this band is fairly efficient for the remote investigation of fine features of disperse media.

It is rather indicative and instructive to compare the frequency properties of the value of extinction (per unit of path) of various disperse media, which are typical for the terrestrial atmosphere (Figure 10.10). Certainly, in this case the question is about the qualitative picture of the phenomenon, and the data presented are not intended

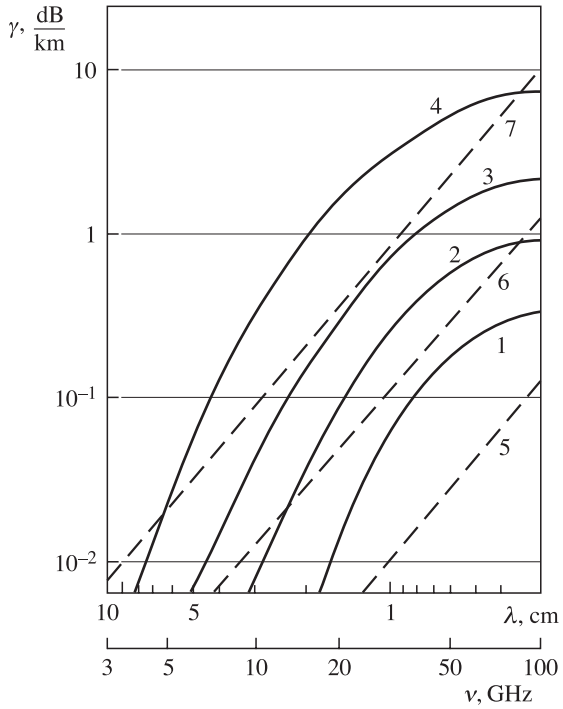

Figure 10.10. Frequency characteristics of attenuation for natural disperse media: rain (solid curves) and fog (dashed curves). Notation is explained in the text.

for quantitative interpretation of particular experiments. The solid lines in Figure 10.10 give the wavelength dependencies of the extinction coefficient for rainfalls with intensities of 0.25 (curve 1), 1.0 (curve 2), 4 (curve 3) and 16 mm/hour (curve 4). According to the existing meteorological classification, these intensities correspond to drizzle, light, moderate and heavy rainfalls. The dashed curves in the figure show the extinction in clouds and fogs, calculated by formula (10.72) for the water content of 0.032 (curve 5), 0.32 (curve 6) and 2.3 g/m^3 (curve 7). These fogs correspond to the visual ranges (in the optical band) of about 600, 120 and 30 m. As follows from the analysis of these data, the picture is rather ambiguous, in general. So, the extinction in a thick sea fog (curve 7) exceeds the extinction in a moderate rainfall (curve 3) in the millimetre and centimetre wavelength bands. And in the long-wave centimetre band the extinction in a thick fog even exceeds the extinction in heavy precipitation. This seems paradoxical, at first sight. However, physically this is associated with a different relationship between contributions to extinction from large-sized (scattering) and small-sized (absorption) drops in various disperse media. So, for the intensive rainfall the frequency dependence of extinction is proportional to $1/\lambda^4$ in the centimetre band, and for the fog to $1/\lambda^2$, which results in an apparent paradox at long centimetre waves.

10.6 FEATURES OF RADIATIVE TRANSFER IN DENSE MEDIA

In connection with the intensive development of microwave diagnostics of composite natural media in the ocean–atmosphere system, it is of interest to study the features of the transmission and scattering of electromagnetic waves in randomly inhomogeneous media with densely disturbed, discrete, highly absorbing scatterers, where the size of particles, the distance between particles, d, and the electromagnetic radiation wavelength, λ, are quantities of the same order. Such important microwave remote sensing tasks include the study of electromagnetic waves scattering and radiation in the cloudy atmosphere with considerable volume densities (more than 0.1%) of hydrometeors (Oguchi, 1983; Nemarich *et al.*, 1988; Lhermitte, 1988), in the drop-spray phase of gravitation waves breaking (Cherny and Sharkov, 1988), in snow–water disperse media (Wen *et al.*, 1990; Boyarskii *et al.*, 1994), in foam-type disperse systems (Raizer and Sharkov, 1981) and in other similar natural media.

With the indicated parameters of a disperse medium the physical conditions of applicability of the radiative transfer theory are obviously violated (see Chapter 9). However, the desirability of using the numerous results of radiative transfer theory doubtless requires, solution of the question on the limits of effectiveness of the theory itself. Certainly, this complicated problem cannot be solved within the framework of radiative transfer theory itself. Its solution is possible either within the multiple scattering framework, or in the experimental way. The theoretical analysis of this problem is far beyond the scope of the present book. Here we shall only describe the results of fine laboratory experiments, which are closest to the subject of the present book, namely, the microwave sensing of dense disperse media. The experiments were carried out during 1976–1986 under the scientific guidance of the author of the present book (Bordonskii *et al.*, 1978; Militskii *et al.*, 1976, 1977, 1978; Raizer and Sharkov, 1981; Cherny and Sharkov, 1988, 1991a,b).

Though there are many experiments studying the electromagnetic properties of tenuous discrete systems with $d \sim (10\text{–}10^4)\lambda$ and volume density $C \sim (10^{-2} - 10^{-4})\%$ (see the review by Oguchi (1983)), no results from studies of electromagnetic properties in the radio-frequency band of dense dynamical media with absorbing scatterers are to be found in the literature. The principal methodological problem in the statement of such experiments lies in the experimental difficulties of producing dynamical dense drop structures with strictly controlled parameters. However, the statement of such experiments is extremely topical, both from general theoretic and from practical points of view. And, first of all, these experiments are necessary for finding the limiting values of densities at which the mechanisms of electromagnetic interaction of solitary absorbing scatterers are 'switched on'. The experiments, carried out in the optical band for transparent media and for semi-transparent particles ('soft particles') have shown (Varadan *et al.*, 1983; Wen *et al.*, 1990), that the essential contribution of multiple scattering falls on the range of densities exceeding 1%, this value of boundary being strongly dependent on the particle size parameter. These numbers cannot, certainly, be directly applied to discrete media with highly absorbing scatterers and can serve

as a quantitative landmark only. The papers by Cherny and Sharkov (1991a,b) contain the results of experimental investigations of characteristics of transmission, backscattering and thermal radiation of millimetre-band electromagnetic waves in a disperse discrete medium with the volume density of spherical scatterers ranging from 0.05% to 4.5%. In this case the average distance, d, between the centers of particles varied within the limits from 2.3 to 0.9λ.

10.6.1 Disperse medium and its characteristics

As we have already noted, the fulfilment of the necessary radiophysical experiments meets with the difficulties of producing, in a free-fall mode, aqueous particles of quasi-monochromatic (in the size spectrum and in the magnitude of velocities) flow with a high density of spherical-shaped particles. On the one hand it is necessary to avoid dynamical deformation and decay of particles of fairly large diametres (of the order of 2–3 mm) and having high velocities of motion (5–10 m/s). On the other hand, the gravitational and turbulent coalescence between drops should not be allowed. The cascade processes mentioned result in a very wide spectrum of particles under natural conditions (in cloudy systems and precipitations, for instance) (see section 10.5). This circumstance, in its turn, essentially hampers the interpretation of the radiophysical experiments. The processes of deformation and decay of drops in a flow are controlled by two dimensionless numbers: the Rayleigh number (for a sphere) $Ra = 2aV\rho\mu^{-1}$ and the Weber number $W = a^2V\rho(2\sigma)^{-1}$. Here V is the steady velocity of a drop; a is the drop radius; ρ and μ are density and viscosity of air; and σ is the surface tension of water. The laminar regime of air flow around drops (the Stokes regime) is kept up to $Ra \approx 300$, and the critical value of W for ensuring the dynamical stability of drops equals 10. The analysis of various methods of forming dense media has led the authors to the conclusion that it is necessary to use a forced regime with a particular flow velocity, rather than a free flow regime. The highly dense disperse medium was produced by averages of a spray system made as a special injector with a removable grid. The grid represents a plate of a particular profile with orifices. The number and diametre of orifices determine the density and size of the drops, whereas the profile determines the value of flow divergence, which also influences the density. The sphericity of drops was specially controlled – the eccentricity of drop ellipses did not exceed 0.3 (for high densities) and 0.1 (for low densities). For the conditions of the described experiment the Ra number was 200 to 300 (for various flow velocities) and $W = 0.03$. Thus, under the experimental conditions both the laminar regime of air flow around a drop (the Stokes condition) was ensured, and the processes of decay and the rise of a wide (decay) spectrum of scatterers was not allowed. If the injector is directed downwards, then the drops, being accelerated under the force of gravity, produce uniform density variation down the flow. Thus, for a single grid it is possible to obtain a wide range of variation of density with the same dispersity (Figure 10.11(a),(b),(c)). The control and measurement of the particle density were carried out by the stereoscopic photography method using two synchronized mirror cameras with telescopic lenses and with a special light flash system (with a flash duration of 10^{-6} s). In addition, the

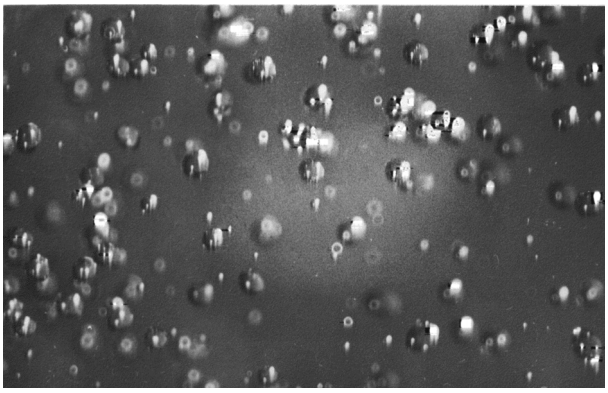

(a)

(b)

(c)

Figure 10.11. Photographs of disperse water drop medium with relative volume concentrations: (a) 0.28%; (b) 1.5%; (c) 4.50%.

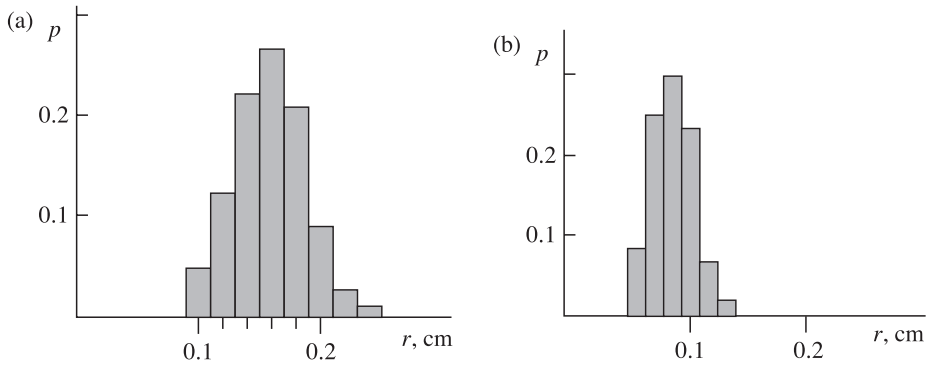

Figure 10.12. The experimental histograms of droplet radii for medium N_1 (a) and for medium N_2 (b).

velocity of drops was measured by the method of tracks (the reflecting blinks on the photo images, Figure 10.11(a)). The operator has analysed the stereo pairs obtained with a stereoscope and, when comparing them with a test-object, determined the number of drops and their disperse properties (at a fixed time instant). The radiophysical measurements were carried out for two types of disperse media whose histograms are presented in Figure 10.12. The form of particle distribution functions $n(r)$ ($\mathrm{dm}^{-3}\ \mathrm{mm}^{-1}$) was approximated by the gamma distribution:

$$\begin{aligned} n_1(r) &= 0.38 N_1 r^9 \exp(-0.73 r^3) \\ n_2(r) &= 73.5 N_2 r^8 \exp(-3.66 r^3) \end{aligned} \tag{10.73}$$

The values of N_1 and N_2 are proportional to the volume density of particles. The average value of radius for medium 1 equals 0.15 cm (and, accordingly, the size parameter $x_1 = 1.18$), and for medium 2 it equals 0.09 cm ($x_2 = 0.7$). The special statistical estimation of fluctuations of the countable particle flux density has shown that the root-mean-square deviation of density was less than 2% (of the average value of N). In this case the samplings, spaced in time from 1 hour to 3 hours, relate to the same general set. It is clearly seen from the analysis of histograms that in forming the dense flux one managed to avoid decay and coalescence processes, and the spectrum of particles could be considered to be close to monochromatic. For these types of media the authors have calculated the extinction, scattering and absorption coefficients in accordance with (10.13), (10.65) and (10.66). In addition, the single-scattering albedo was calculated for the unit volume of a polydisperse medium, using the function of size distribution of particles obtained from the experiment. The calculations were carried out for the working radiation wavelength $\lambda = 8$ mm and the complex index of refraction of water $m = 5.39 - \mathrm{j}2.81$, which corresponds to the water temperature $t = 22^{\circ}\mathrm{C}$ and salinity $S = 0‰$. By virtue of the fact that the tenuous medium approximation with a near-monochromatic spectrum is used here (see relations (10.67) and (10.68)), the scattering albedo for

the unit volume of a medium will correspond to the value of albedo of a solitary particle (so, for medium N_1 $\omega = 0.63$, and for medium N_2 $\omega = 0.43$) and will not depend on the medium density.

10.6.2 Experimental technique

The purpose of the experiment was to measure the radiophysical characteristics of a disperse dynamical medium with strict control of the disperse medium parameters. The measurements were carried out in three modes: bistatic (radiation transmission through the medium within the line-of-sight limits), scatterometric (backscattering investigation) and radiometric. The extinction of the medium was measured in the first version, the backscattering cross-section in the second one and thermal radiation of a disperse medium in the third version. The fluctuations of scattered radiation intensity were measured along with its average values. The extinction, absorption and scattering coefficients, the scattering and backscattering albedo (in the 'cold' layer approximation) and the thermal radiation of a disperse medium with a spherical scattering indicatrix were calculated using the analytical solution of the equation for a plane-parallel layer (in the 'pure' absorption approximation).

10.6.3 Average values of electrodynamical characteristics

Comparing the experimental and theoretical values of extinction and thermal radiation for the disperse medium 1 (the average diametre of particles was 0.3 cm), we can see the distinction, which is noticeably revealed with increasing density of particles (Figure 10.13). One can distinguish the region of low deviation of experimental from theoretical data and the region of greater deviation. The boundary that separates these regions corresponds to a value of particle volume density approximately equal to 0.8%, this boundary being the same both for extinction and for thermal radiation. Considering the results of investigation of the extinction value for disperse medium 2 (where the average diametre of particles was 0.2 cm), we can see that the aforementioned boundary lies in the region of particle volume density values of 0.15%. Now we shall analyse the dependence of extinction values for a disperse medium on the number N of particles in a unit volume (the countable density), rather than on the particle volume density C. It can be seen from Figure 10.13 that in this case the boundaries mentioned lie in the range of $N_0 = 500$–$550\,\mathrm{dm}^{-3}$ for both types of disperse medium. That is, they virtually coincide. In its turn, quantity N_0 determines the average distance between particles as $d \sim N^{1/3}$. Therefore, now we can characterize the aforementioned boundary by the distance between particles, i.e. by $d \sim 1.5\lambda$.

Thus, from the analysis of experimental data and from theoretical calculations it follows, that the radiative transfer theory in the tenuous medium approximation satisfactorily describes electromagnetic properties (the average values) of a discrete disperse medium with absorbing scatterers, provided that the distance between particles $d > 1.5\lambda$. In the case where $d < 1.5\lambda$, the experimental data principally differ from calculated data. For example, for the particle volume density

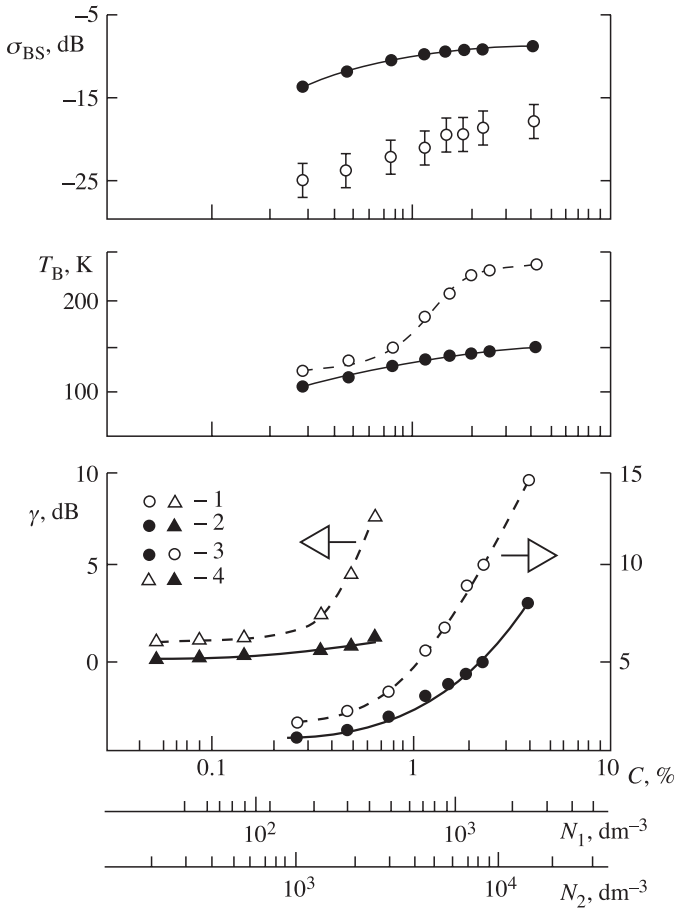

Figure 10.13. The extinction coefficient (γ), radiobrightness temperature (T_B) and backscattering cross-section (σ_{BS}) of disperse water drop media as functions of the volume concentration (C) and the number density (N): (1) experimental data; (2) theoretical results; (3) data for medium N_1; (4) data for medium N_2.

$C = 4.5\%$ ($d = 0.9\lambda$) the distinction for the radiobrightness temperature equals 86 K, and for the extinction value −6.5 dB. As far as the backscattering is concerned, here the experimental and theoretical data (in the cold layer approximation) essentially (by about 10 dB) differ throughout the range of particle densities. Now, using the experimental data, we shall estimate the disperse medium parameters for the particle volume density value $C = 4.5\%$ ($d = 0.9\lambda$).

The electrodynamical parameters have been estimated by means of a specially developed technique of complex combining the data of active and passive measurements for the same investigated medium (Cherny and Sharkov, 1991a). In this case the expressions for radiobrightness temperature were obtained in the 'pure' absorption approximation (see Chapter 9). It is important to note that the

inclusion of the integral term into the transfer equation that describes the 'internal re-scattering' in a layer does not essentially change the spectral characteristics of a medium in the case of absorbing scatterers considered. This follows from the comparison of calculations with the results of solving a similar problem by the double spherical harmonics method and by the Monte Carlo method. Of importance is the fact that, for indicated values of density of particles in a medium, the electrodynamical parameters of a disperse medium have essentially changed as compared to calculated values (for a tenuous medium) obtained in the single-scattering approximation. So, the scattering albedo of a unit volume of disperse medium N_1 decreased three times (from the value of 0.63 down to 0.22). The extinction and absorption coefficients, on the contrary, increased about 1.5 times (from the value of 0.63 up to $0.94\,\mathrm{cm}^{-1}$) and three times (from the value of 0.23 up to $0.73\,\mathrm{cm}^{-1}$), respectively. And the scattering coefficient value decreased twice in this case (from the value of 0.40 down to $0.21\,\mathrm{cm}^{-1}$). The result considered indicates that for the disperse dense medium with absorbing scatterers the interaction of particles results, primarily, in growing absorption in a medium and, therefore, in increasing its thermal radiation and, in addition, in decreasing scattering properties of a medium.

10.6.4 Fluctuation mode of extinction

It is important to note that in the same paper Cherny and Sharkov (1991a) have demonstrated experimentally the principal change of the character of the fluctuation mode of extinction in a dense medium. This effect is visually illustrated in Figure 10.14, which presents the registograms of an external harmonic signal transmitted through the medium, this signal being considered at an intermediate frequency. The fluctuations of intensity of transmitted radiation are observed in the form of mirror-symmetrical amplitude modulation of the signal. The measurements were carried out with extinction recording by exposure to microwave radiation. It can easily be seen that the statistical characteristics of a signal sharply change in the case of two distinguishing densities. One of the possible physical causes, explaining fluctuations of radiation transmitted through a medium, could be associated with changing the countable number of particles in the volume under study. We shall indicate, however, that this is not the case.

So, we shall consider, for example, in accordance with the Bouguer law, the ratio of intensities of external radiation, weakened by a medium, for different time instants

$$(I_1/I_2) = \exp(\tau_2 - \tau_1) \tag{10.74}$$

or

$$\tau_2 - \tau_1 = \ln(I_1/I_2), \tag{10.75}$$

where τ_1 and τ_2 are opacities of an investigated disperse medium at different time instants. Since in the single-scattering approximation for a medium with a monochromatic spectrum of particles we have $\tau = Q_{\mathrm{E}}\pi r^2 Ns$ (here s is the linear size of a medium), one can write the following finite-difference relation:

$$(\Delta N/N) = (\Delta\tau/\tau) = (1/\tau)\ln(I_1/I_2). \tag{10.76}$$

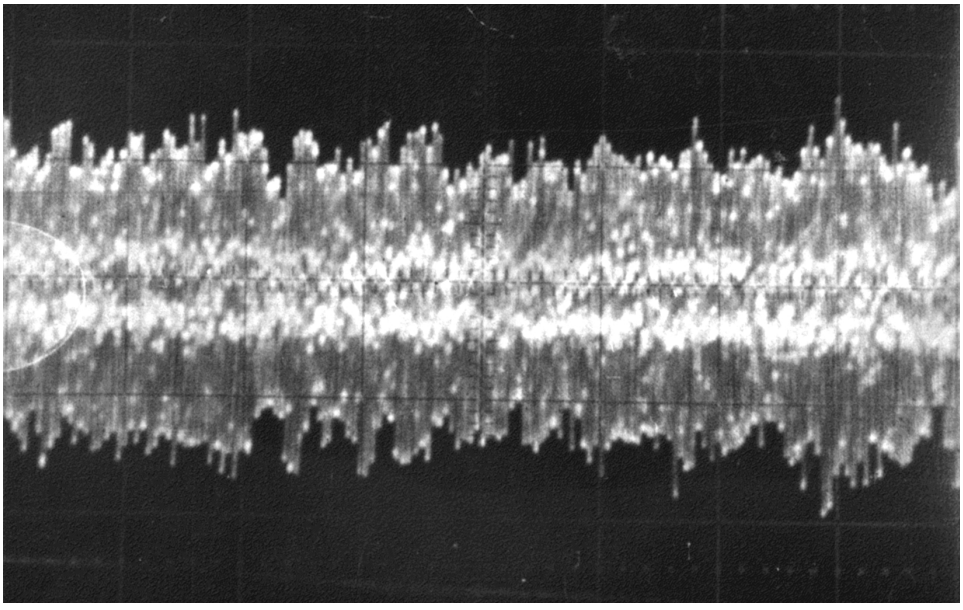

(a)

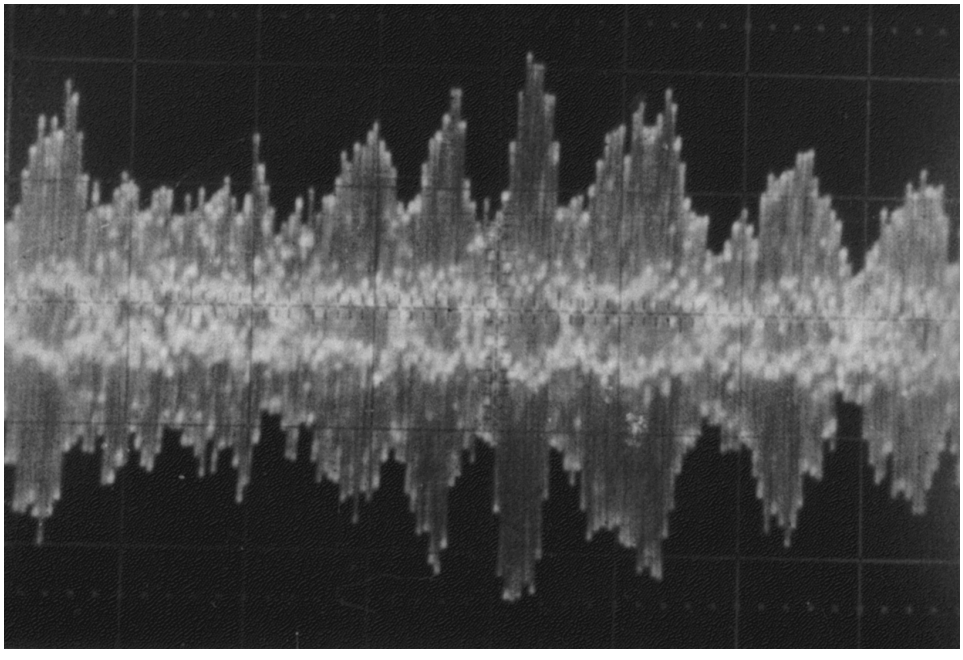

(b)

Figure 10.14. The photographic registrograms of a signal (at intermediate frequency) transmitted through a water drop medium with volume concentrations 0.28% (a) and 4.5% (b).

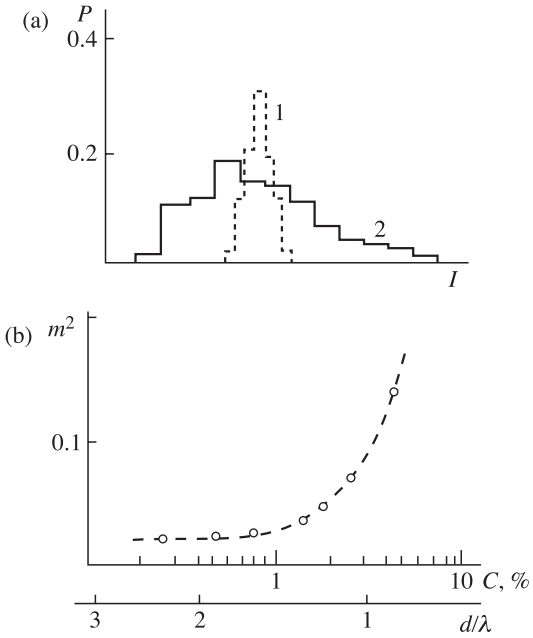

Figure 10.15. The statistical characteristics of radiation intensity of a signal transmitted through a water drop medium: (a) the density function (experimental histograms) with two volume concentrations: (1) 0.28%; (2) 4.5%; (b) the scintillation index m^2 as a function of the volume concentration and of the distance between particles.

Proceeding from this relation, we shall estimate the maximum value of $(\Delta N/N)$ for the volume density of particles of a disperse medium $C = 4.5\%$, at which $(I_{\max}/I_{\min} = 6.1$, and the quantity $\tau = \gamma/4.34 = 3.34$ represents the average value of opacity. Substituting this value into (10.76), we find $(\Delta N/N) = 54\%$, but this is impossible, since the particle density fluctuations in a disperse flow do not exceed 2% with the probability of 0.95. Thus, a sharp growth of the variance of fluctuations of a medium's extinction are not determined by fluctuations of the number of particles in the flow, but has another physical nature.

We pay attention to the principal point that, as the density of particles increases, the character of fluctuations also changes. So, the probabilistic distribution of intensity of a signal, transmitted through the investigated medium at $C = 0.28\%$, has a prominent normal character, whereas at $C = 4.5\%$ the intensity fluctuations are distributed according to the normal logarithmic law (Figure 10.15). This circumstance is clearly exhibited on registograms in visual observation as well (Figure 10.14). For the mentioned volume density values and, accordingly, for $(d/\lambda) \sim 1.5$ the so-called scintillation index sharply increases (Figure 10.15(b)). The latter characteristic is often used in optical observations, which gave rise to the term. However, the mentioned characteristics do not provide a detailed picture of the distribution of fluctuations over the scales of interactions (see Chapter 2). Let

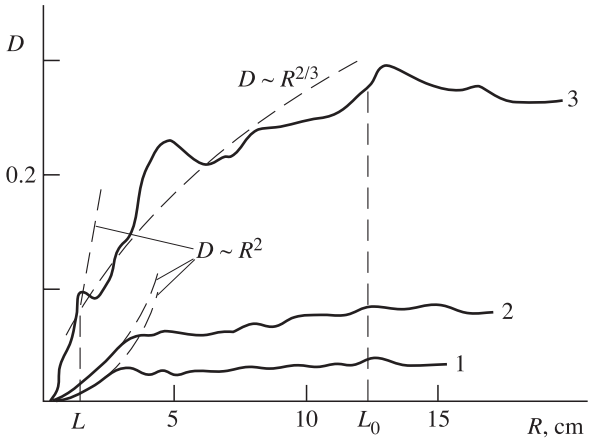

Figure 10.16. The structure function of intensity fluctuations for a signal transmitted through a water drop medium with three volume concentrations: (1) 0.28%; (2) 1.5%; (3) 4.5%.

us consider the behaviour of a structural function expressed in terms of spatial coordinates. The transition from spectral–temporal coordinates t and f to a spatial-frequency presentation of R and k (the spatial–wave number) (see Chapter 5) can be accomplished based on the hypothesis of 'freezing' inhomogeneities in a moving flow:

$$R = Vt, k = \frac{2\pi f}{V}, \tag{10.77}$$

where V is the particle flux velocity in the direction perpendicular to radiation transmission. Figure 10.16 presents the structural function of intensity fluctuations for three values of volume density of a disperse medium. Now we shall analyse the behaviour of a structural function, which represents the mean square of the magnitude of an increment of the fluctuation component $I(R)$ of intensity $I(R)$ (Rytov *et al.*, 1978):

$$D(R_1, R_2) = \langle |I(R_1) - I(R_2)|^2 \rangle. \tag{10.78}$$

If the studied spatial field has the character of locally homogeneous one, i.e. depending only on the difference of scales of interactions $R = R_1 - R_2$, then the form of a structural function can be essentially simplified:

$$D(R) = 2[B(0) - B(R)], \tag{10.79}$$

where $B(R)$ is the spatial correlation function (see Chapter 2 and 5). The important property of a structural function consists in the fact that it excludes from consideration the large-scale inhomogeneities L_0. In our case the latter represent the characteristic size of a particle flux. The correlation function takes into account fluctuations of any scale in equal measure. For this reason the use of a structural function is physically justified in those cases where we are interested in the fluctuations on scales much smaller than L_0.

For $C = 0.28\%$ and $C = 1.5\%$ the rapid saturation of a structural function takes place on scales of the order of $R = 3\,\text{cm}$. For $C = 4.5\%$ the form of a structural function essentially differs from previous cases. Here both the internal ($l_0 = 1.5\,\text{cm}$) and the external ($L_0 = 12\,\text{cm}$) scale of inhomogeneities is clearly exhibited, and in the interval of $l0 < R < L_0$ the structural function grows as $D \sim R^{2/3}$. The limiting value of a structural function (in the saturation region) is equal to a double value of the variance of fluctuations.

Thus, the analysis shows that for the volume density of particles $C = 4.5\%$ ($d = 0.9\lambda$) the scattering of electromagnetic radiation in a medium occurs on spatial inhomogeneities whose scale lies in the interval between $l_0 = 1.5\,\text{cm}$ and $L_0 = 12\,\text{cm}$, which is much greater than the size of particles (the diametre is 0.3 cm) and the distance between them ($d = 0.7\,\text{cm}$). This fact, in its turn, confirms the existence of collective effects in scattering. The circumstance that the intensity fluctuations are distributed according to the normal logarithmic law and the spectrum of fluctuations and a structural function can be described by well-known exponential laws of '$-5/3$' and '$2/3$', respectively, indicates to the turbulent-vortex character of fluctuations with quasi-vortex inhomogeneities. Therefore, the discrete disperse medium for $d < \lambda$ can be considered to acquire the properties of a continuous randomly inhomogeneous medium, in which the spatial fluctuations of dielectric permittivity take place (Rytov *et al.*, 1978).

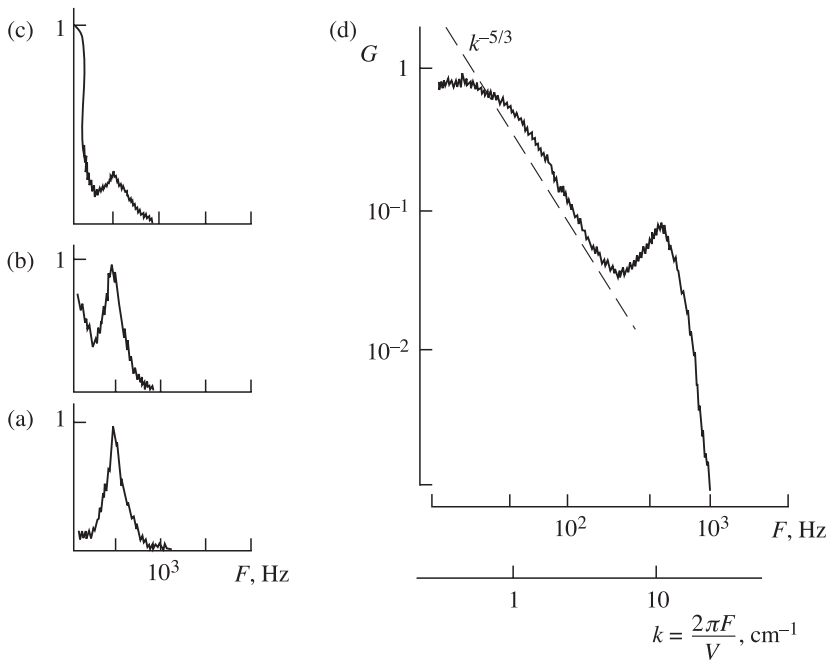

Figure 10.17. Normalized Doppler spectra of backscattering signal from a disperse medium with three volume concentrations: (a) 0.28%; (b) 1.5%; (c) 4.5%; (d) 4.5% in bi-logarithmic coordinates. $V_D = 1.7\,\text{m/s}$; $V = 2\,\text{m/s}$.

Consider now the results, obtained by means of the Doppler scatterometre, in the mode of observation of microwave radiation backscattering by the same disperse medium (Cherny and Sharkov, 1991b). Figure 10.17 presents the Doppler spectra of a scatterometric signal backscattered by a disperse medium. The measurements were carried out in such a manner that the moving flux of particles had a velocity component in the direction of the instrument. As a result, the power of radiation scattered by particles lies in the spectrum of a scattered signal at the Doppler frequency f_D determined by the velocity component in the direction of instrument $f_D = 2v_D/\lambda$, which is clearly seen for the particle volume density $C = 0.28\%$. However, as the particle density grows (Figure 10.17(b),(c)), the form of a spectrum essentially changes and, along with the Doppler components, the additional component appears in the spectrum, which is concentrated near 'zero' frequencies (for $C = 4.5\%$). The appearance of 'zero' frequencies in a spectrum in the case of moving scatterers can be physically related to the loss of temporal coherence of the scattered signal. This makes impossible the phase detection of a signal with the purpose of obtaining information on the object velocity based on the Doppler effect.

The presentation of results in the bilogarithmic coordinate system (Figure 10.17(c)) reveals an interesting point – the spectrum of an 'incoherent' component obeys the exponential law of '$-5/3$' in the frequency band of 20–200 Hz. Moreover, the range of spatial frequencies k, where the spectrum obeys the '$-5/3$' law in the backscattering mode, is exactly the same as in the case of radiation transmission within the line-of-sight limits (by exposure to microwave radiation) (see Figure 10.16). It can be supposed that, both in the bistatic and in the scatterometric mode of measurements, the fluctuations of intensity have an identical nature. The exponential law in the spectrum of scattering, as well as the gamma distribution of intensity amplitudes, can be treated as the result of scattering from the fractal, geometrically bound structure (or from a turbulent-vortex space) in a volume body of discrete flow (Lakhtakia *et al.*, 1987; Varadan *et al.*, 1983).

The analysis of calculated and experimental data indicates that there exists a quite specific (critical) value of the distance between absorbing scatterers ($d/\lambda \leq 1.5$), which makes a basic rearrangement of both average values of electrodynamical parameters, and the fluctuation mode.

It is of interest to compare the experimental results with the electrodynamically closely dense medium condition, obtained theoretically in the book by Rytov *et al.* (1978):

$$n\alpha \geq 1, \tag{10.80}$$

where n is the average density of scatterers and α is the polarizability of particles, which in the Rayleigh approximation is equal to

$$\alpha = r^3|(\dot{\varepsilon} - 1)/(\dot{\varepsilon} + 2)|, \tag{10.81}$$

where e is the complex dielectric constant of the scatterer's material. Condition (10.80) describes physically the contribution of induced dipoles, closest to an

original particle, to the effective field. So, taking into account, for a critical value of $d = 1.5\lambda$, $n \approx 2.6\,\mathrm{cm}^3$, we have

$$n|\alpha| = 1.2 \times 10^3 \ll 1.$$

Thus, long before satisfying the condition (10.80) the dense discrete medium basic changes its properties and becomes similar, in a certain sense, to a continuous medium with fluctuating parameters.

It is interesting to note that seemingly similar physical structures (a set of hollow aqueous spheres) manifest themselves, however, in a quite opposite manner: even a compact, dense packing of scatterers of such a type does not make any noticeable contribution to the electrodynamics of a system, owing to a very weak effect of interaction between single structures. Each of hollow aqueous spheres represents an almost black-body emitter, which does not possess any noticeable scattering properties and does not interact with surrounding components of a system (Raizer and Sharkov, 1981).